TISSUE ENGINEERING: Part B
Volume 25, Number 3, 2019
Mary Ann Liebert, Inc.
DOI: 10.1089/ten.teb.2018.0284

termis
Tissue Engineering
& Regenerative Medicine
International Society

***REVIEW ARTICLE***

# Biomimetic Designer Scaffolds Made of D,L-Lactide-ε-Caprolactone Polymers by 2-Photon Polymerization

Nicole Hauptmann, PhD, Qilin Lian, MSc, Johanna Ludolph, MSc, Holger Rothe, MEng, Gerhard Hildebrand, PhD, and Klaus Liefeith, PhD

Traditionally tissue engineering (TE) strategy relies on three components: cells, signaling systems (e.g., growth factors), and extracellular matrix (ECM). Nowadays the combination of cells, signaling systems, an artificial ECM, and appropriate bioreactor systems has recently been defined as the ''Tissue Engineering Quadriad'' taking into consideration the fundamental role of the dynamic physiological environment. Not surprisingly, the establishment of an artificial ECM with the necessary flexibility seems to be a mission impossible without advanced materials and fabrication techniques. This claim applies to therapeutic (regeneration) as well as diagnostic (disease-modeling) approaches. To meet the challenge to mimic the hierarchical structured and complex milieu of the natural ECM it was tried in this study to combine a flexible photosensitive polymer platform based on (D,L)-lactide-ε-caprolactone methacrylate (LCM) with a nanoscale rapid prototyping technique based on two-photon polymerization (2-PP). Polyesters, such as poly-ε-caprolactone or poly-(D, L)-lactide, are very popular candidates for mimicking the ECM, because of their adjustable biophysical and biochemical properties. 2-PP represents a versatile lithographic method for the generation of scaffolds with defined size and shape, due to a spatial resolution <100 nm. This unique performance enables the fabrication of mathematically defined structures (scaffolds) based on triply periodic minimal surfaces with a tailor-made stiffness, permeability, and degradation behavior. Especially the Schwarz P minimal surface, which divides the interior of a scaffold into two intertwining labyrinths, plays an important role in generating custom-made or designer scaffolds. This review gives an overview of materials, techniques, and appropriate geometries to establish a conceptual framework to engineer such scaffolds. Furthermore, selected application scenarios in bone and tumor TE were introduced in the sense of a first proof of principle to show the high potential of this concept in therapeutic (regeneration) and diagnostic (disease-modeling) approaches.

**Keywords:** 2-photon polymerization, polymeric scaffold, tumor microenvironment, bone, lactide, caprolactone

### Impact Statement

In tissue engineering (TE), the establishment of cell targeting materials, which mimic the conditions of the physiological extracellular matrix (ECM), seems to be a mission impossible without advanced materials and fabrication techniques. With this in mind we established a toolbox based on (D,L)-lactide-ε-caprolactone methacrylate (LCM) copolymers in combination with a nano–micromaskless lithography technique, the two-photon polymerization (2-PP) to mimic the hierarchical structured and complex milieu of the natural ECM. To demonstrate the versatility of this toolbox, we choose two completely different application scenarios in bone and tumor TE to show the high potential of this concept in therapeutic and diagnostic application.

Department of Biomaterials, Institute for Bioprocessing and Analytical Measurement Techniques e.V. (iba), Rosenhof, Heilbad Heiligenstadt, Germany.

## Introduction

Tissue engineering (TE) has been recognized as an interdisciplinary approach to establish functional substitutes to restore, maintain, or improve the function of diseased or damaged human tissue compartments and organs as an important future therapeutic option. To meet the current clinical requirements in view of functional TE, the combination of cells, signaling systems, an artificial ECM, and appropriate bioreactor systems has been defined as the ''Tissue Engineering Quadriad.''[1] In parallel, numerous chip technologies (organ-on-a-chip, tissue-on-a-chip, human-on-a-chip, etc.) came up recently to reduce or replace animal testing and to enable disease-modeling strategies as equally important diagnostic options. In the meantime the extent of possible clinical applications includes nearly all tissues and organs of the human body such as hard and soft TE, cardiovascular TE, skin TE, and three-dimensional (3D) tissue models to study organ-specific regeneration[2–5] and disease processes of various pathologies such as cancer to name one of the most important societal challenges.[6]

There is no doubt that all these innovative approaches require a new quality of biomaterials to be able to recreate a complex 3D architecture to mimic the environment of the natural ECM for the particular cell type which is under consideration (site specificity). In other words, this means that 3D biomaterial constructs must be developed to provide a more or less temporary mechanical support to interact with the cells on different hierarchical levels to regulate their proliferation, differentiation, and migration until the regeneration process is completed.[7,8]

In this study the attempt is made to introduce and to validate an extended photosensitive copolymer system (D,L)-lactide-ε-caprolactone methacrylate (LCM) in combination with a direct and maskless laser writing process based on 2-PP using mathematically precisely defined TE scaffolds. The validation of our strategy to prepare any such ''designer scaffolds'' was performed for two completely different clinical application scenarios: (1) bone TE and (2) tumor TE for breast cancer research. Figure 1 summarizes already established application fields of 3D constructs in regenerative medicine taking into consideration any implants for bone reconstruction,[2–4] artificial cartilage,[9–11] or systems for tumor TE.[12–14]

In the past, a huge number of studies focused on two-dimensional (2D) substrates, but these 2D techniques ignore the fact that cells grow in three dimensions. Thus, several 3D cell culture systems, such as spheroids, polymer matrices, or autologous tissues, were used to simulate cell proliferation and differentiation. Spheroids are 3D cell aggregates that can be generated by force floating, hanging drop, or agitation-based methods. These cell aggregates are easy to use and the preparation methods are relatively simple, but the creation of homogeneous spheroids is quite difficult.[15] It must also be highlighted that the dimension of the cell aggregates is limited because of the formation of a necrotic core, which is due to the limited supply of nutrients and transport of metabolites.[16] Thus, spheroids failed to replace larger tissue defects.

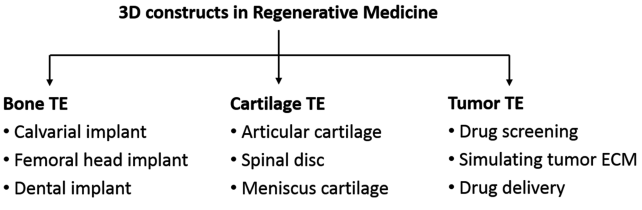


**FIG. 1.** Overview of application areas of three-dimensional constructs in regenerative medicine.

When creating artificial tissues, two main conditions have to be considered: (1) the hierarchical structure of biological tissues and (2) the site-specific stiffness of the damaged tissue, which must be replaced by an artificial 3D construct. Especially, the stiffness seems to be much more important than assumed in the past when reconstructing the native environment of bone or tumor tissue. While implants for bone reconstruction possess a well-known and defined stiffness range (cancellous bone: 100–500 MPa, cortical bone: 12–18 GPa), tumor tissue is comparably heterogeneous (Fig. 2). The stiffness of tumor tissue ranges from 1 kPa until 1 MPa, whereas the peripheral surface region seems to be stiffer than the interior of the tumor obviously due to collagen reorganization and capsule formation.[17]

Due to the observed stiffness heterogeneity, it would be of advantage to introduce a scaffold-based cell culture system with tunable mechanical properties. One very interesting option to fulfill any such claim is the utilization of a suitable copolymer system that allows the variation of the monomer ratio and the synthesis process to tailor-made mechanical properties in accordance with the relevant *in vivo* situation. These 3D matrices do not have the above-mentioned limitations of 2D substrates or spheroids, and the mechanical properties are adjustable by the variation of the chemical structure (chain length) or the crosslinking degree. In several studies, it was shown that these porous structures with adapted stiffness properties could be used in various applications, among others for bone and cartilage TE or for the simulation of the tumor microenvironment.[9,14,18] These scaffolds are characterized by a high degree of interconnectivity for nutrient supply and the transport of metabolites, a pore size that enables tissue ingrowth, ECM analog surface chemistry for increasing cell attachment, a suitable degradation rate,[15] and a certain potential to guide the multicellular and spatiotemporal process of tissue regeneration.

Keeping all this in mind, it can be concluded that the ideal scaffold for tumor TE in breast cancer research should have variable mechanical properties from 50 kPa until 500 kPa, pore sizes of 100–300 μm, sensitive peptides for integrin-mediated cell adhesion (RGD), and protease-based matrix degradation matrix-metallo-proteinase.[6,19] It is of value to point out that in other studies on prostate cancer published recently, hydrogels were used with Young's modulus of 330 Pa and a pore size of *130 nm.[20] In contrast to that, scaffolds for bone reconstruction should be significantly stiffer (Young's modulus 50–100 MPa), with pore sizes of 300–500 μm and superficially immobilized peptides for integrin-mediated cell adhesion (RGD) and template-associated mineralization (GGGSRGD).[21,22] The degradability should be tailor made according to the increasing loading capacity of the healing bone tissue.

For the development of scaffolds, various methods were established such as solvent casting/particulate leaching, gas foaming, freeze drying, thermally induced phase separation, textile technologies (electrospinning), or powder forming techniques and sol–gel techniques. In general it can be concluded that these conventional techniques possess several drawbacks such as an inadequate degree of continuous interconnectivity and irregular pore morphology. Furthermore distribution, size, and geometry of pores can often not

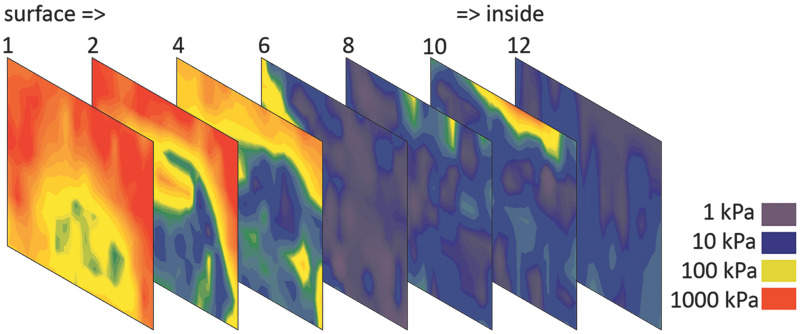


**FIG. 2.** Stiffness mapping of sections of mamma carcinoma measured by nanoindentation from the peripheral region (*left*) to the central region (*right*), *red*: stiff, *purple*: soft, 500 µm sections.

precisely be controlled, and these techniques suffer frequently from a poor reproducibility.[16,23]

To overcome these disadvantages ''Solid Freeform Fabrication (SFF) techniques or rapid prototyping (RP) techniques were introduced, which allow the fabrication of very complex components based on computer data prevalently by means of a Layer-by-Layer (LbL) strategy.

A detailed description of the numerous methods is beyond the scope of this study. Interested readers are referred to recently published review articles for in-depth discussions.[16,23,24]

Within these SFF methods, the so-called 2-PP occupies a special position due to the unique combination of nanoscale resolution and inherently 3D fabrication ability.[25] This method represents a photolithographic technique, which enables 3D direct and maskless laser writing of various photoresists.[26] For the two-photon process ultrafast pulses of a near-infrared femtosecond laser are used to achieve the necessary photon flux. The laser light is focused by an objective to a defined focal point in the sample. Due to the simultaneous absorption of two photons by the photoresist and the nonlinear character of the two-photon absorption process, the photochemical reaction occurs only in the focal volume of the laser beam.

Due to the movement of the laser focus relative to the sample or vice versa, 3D structures with defined architectures can be generated.[21] For 2-PP, infrared (IR) transparent, highly viscous methacrylated or acrylated polymers or biopolymers[25] can be used, such as polycaprolactone,[26] polylactide,[27] polyethylene glycol (PEG),[28] hyaluronic acid,[29] or gelatin.[30] Because of the wide field of medical devices such as bone grafts, synthetic cartilage, or artificial ECMs, the mechanical properties of the 3D construct should be tunable over some orders of magnitude.[31] In detail this means that 2-PP processing allows the generation of scaffolds with defined mechanical strength (1) by using special photosensitive and IR-transparent polymer systems, and (2) by optimizing structuring parameters such as slicing, hatching, and writing speed.[32] In summary, 2-PP enables the generation of scaffolds with mathematically defined size and shape, interconnected pores, high porosity, and tunable mechanical and degradation properties at a resolution in the nanometer range. Thus, it can be concluded that 2-PP is a versatile technique for generation of ''designer scaffolds'' in TE.

## Materials Used for Scaffold Production

### *Synthetic polymers versus natural polymers*

For the establishment of artificial matrices using photopolymerization, the material selection is of enormous importance. From a chemical point of view the polymer should possess an appropriate IR transparency and viscosity, as well as an optimal polymerization ability and a low shrinkage or a tolerable degree of swelling. Furthermore, the polymeric material should fulfill various biomedical requirements such as biocompatibility, nonimmunogenicity, and stability against mechanical forces. Depending on the field of application, the biomaterial should have an appropriate degradation time, and the degradation products should not show any toxic effects. These are the reasons such a huge variety of biomaterials were introduced for the establishment of artificial ECM's and devices for cell cultivation.

Materials that were used for scaffold production can be subdivided into synthetic polymers, natural or biological polymers, and hybrid materials (Fig. 3). For establishment of synthetic polymers for regenerative medicine the main focus lies on poly-(D, L)-lactide (PLA),[33,34] poly-ε-caprolactone (PCL),[35,36] poly-L-glutamic acid (PGA),[37,38] PEG,[39,40] or copolymers/blends made of these polymers.[41,42] The use of synthetic polymers has the advantage that these materials are characterized by strictly defined biophysical and biochemical properties. Thus, the mechanical strength of the material correlates with the degree of polymerization, the chain length, and of course the intrinsic swelling/shrinkage properties. It was also shown that scaffolds fabricated from PLA, PGA, or PCL degrade in a time-dependent manner.[43]

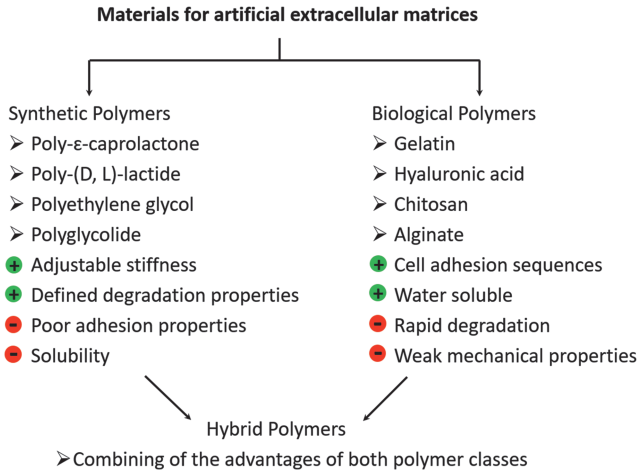


**FIG. 3.** (Bio-) polymers for establishment of designer scaffolds.

An often-used polymer for bone TE is the aliphatic polyester PCL due to its excellent biocompatibility and physical properties as well as its inherent biodegradability. Furthermore, it was shown that PCL scaffolds initiate an increase in revascularization and was characterized by osteoinductive/osteoconductive properties. Owing to its specific chemical structure, PCL degrades in two steps: first, there occurs an enzymatic splitting of the ester bonds, which leads to reduction of the viscosity and the molecular weight. Then a chain splitting occurs, followed by fragmentation of the material and intracellular degradation.[35,44] The suitability of PCL for bone regeneration was also demonstrated in a study, where an injectable and crosslinkable biomaterial based on PCL and hydroxyl apatite was established for bone and nerve regeneration. A crosslinked network was shown to build up both crystalline and amorphous regions. The degree of crystallinity and the melting temperature are adjustable through variation of the molecular weight. In addition, the mechanical properties and hydrophilic properties are highly dependent on the molecular weight of the polymer. Interestingly, the material with the highest crystallinity showed the best cell spreading properties.[45] In several studies, block copolymers or polymer blends consisting of PCL and a more hydrophilic polymer were used to verify the physical and biological properties.

Huang *et al.* synthesized PCL/PEG diblock and triblock copolymers, and analyzed the degradation of the material.[43] Using PEG polymer blends can be advantageous due to the hydrophilic and very good swelling properties of PEG. Thus, transport of nutrients and metabolites is increased in a hydrophilic matrix in comparison with a more hydrophobic one.[46] Nevertheless, the antiadhesive properties of PEG make it difficult to increase the amount of PEG in the polymer blend without decreasing the cell attachment properties. In a study of Vertenten *et al.* D, L-lactide-ε-caprolactone copolymers were synthesized for their use in bone regeneration. The material showed excellent biocompatibility and moderate osteoconductive properties.[47]

Another class of polymers for scaffold production derives from natural sources, such as animal skin, crustacean, or algae.[48] Thus, biopolymers such as collagen,[49] gelatin,[50] hyaluronic acid,[51] chitosan,[52] or alginate[53] were chemically modified, and fabricated to artificial 3D constructs of different dimensions and shapes. Using natural polymers in TE can be advantageous due to their high biocompatibility, good biodegradability, nonimmunogenic properties, and molecular structure, which includes peptide sequences for cell adhesion and other. Biopolymers also consist of nearly the same micro- and nanodimensions, like the fibrous structure of the native ECM.[54] Main disadvantages of this kind of material are the poor mechanical properties, batch-to-batch variations, low reproducibility, and rather complicated isolation protocols. This leads to a limited application field of these polymers.[55] Several studies tried to increase the mechanical properties of scaffolds made from biological molecules. It was demonstrated that mixing of alginate to collagen can enhance Young's modulus between 4 and 26 kPa.[56] Nevertheless, it is very difficult to produce stable biopolymer scaffolds, because of the small amount of photosensitive groups and the long polymer chains between reactive moieties.

Another interesting option when searching for an ideal material for scaffold production seems to be a combination of naturally derived polymers with the properties of the synthetic polymers. Thus, generating a mechanically stable polymer backbone with natural cell adhesion and/or proteolytic sequences and defined degradation properties could be a suitable strategy to develop an ideal hybrid 3D construct for regenerative medicine. Numerous excellent approaches to establish hybrid scaffolds such as blending or coating methods were published recently. Chan *et al.* developed polymer blends based on alginate and a triblock copolymer consisting of PGA, poly (ethylene oxide), and poly (propylene oxide). Crosslinking occurred by physical interaction of calcium ions with the glucoronic acid of the alginate, followed by chemical crosslinking by radical polymerization. The results demonstrated reduced swelling, increased mechanical strength, and an improved degradation rate.[53] Chitosan-g-oligo-(D, L)-lactide copolymers were established as scaffold materials for drug delivery and wound healing applications. Through covalent coupling of hydrophobic lactide side chains to chitosan, an amphiphilic structure was generated with adjustable properties such as biocompatibility, degradation rate, and mechanical properties.[57] Methacrylated chitosan and PEG-dimethacrylate were also used for the generation of mechanical stable hydrogels with an elastic modulus between 1 and 10 kPa.[58] The same research group established hyaluronic acid-poly(ethylene glycol) diacrylate hydrogels with quite strong mechanical properties in the range of 30 kPa until 450 kPa.[29] Kumbar *et al.* designed mechanical stable scaffolds based on cellulose polysaccharides for bone healing application. The scaffolds had a porosity and a stress–strain behavior similar to native bone.[59]

### *Establishing materials with defined mechanical properties*

It is worth mentioning that natural polymers were applied successfully in numerous clinical applications; however, we must state that especially the increased need of organ-specific matrices for regeneration and disease modeling drives the development of custom-made or designer scaffolds with a tissue-specific architecture and bioactivity using synthetic polymers.[8] Furthermore, increasing evidence is emerging on the mechanical role of the microenvironment of cells and the resulting ECM–cell interactions. It is widely accepted that mechanical signals have profound effects on cellular functions, including growth, differentiation, apoptosis, motility, and gene expression.[60] Consequently, the selected material platform should enable the synthesis of copolymers with tailor-made mechanical properties and degradation characteristics by controlling the chemical composition and architecture of the crosslinkable oligomers.[61,62]

In bone TE a compromise between stiffness and flexibility should be achieved, leading to a relatively stiff material with adequate elastic properties.[63,64] Scaffolds for the simulation of the tumor microenvironment should notably be very soft due to the fact that the stiffness of the tumor microenvironment affects the differentiation of tumor cells to a more invasive phenotype.[65] Furthermore, it is known that cells ''feel'' the stiffness of their environment by change of the spreading area, cell shape, cytoskeletal orientation and organization. So, it was already shown that spreading area of cells increased when increasing Young's modulus from 100

Pa to 100 kPa.[66] This effect is called mechanosensing, and describes essentially the fact that cells are able to sense when a mechanical force is applied to them. Various cell membrane receptors contain extracellular domains that bind to the various proteins of the ECM and enable a corresponding cell response (membrane channel activity, up- or downregulation of gene expression, alterations in protein synthesis, adapted cell morphology) through a variety of biological pathways.

It is important to note that two aspects should be discussed independently from each other: the behavior of the cell against the stiffness of the environment (mechanotransduction) and the force generated by the cell itself, which can lead to cell-specific proliferation and differentiation processes. Interestingly, changes in tissue stiffness during tumorgenesis or fibrosis are not epiphenomena of the disease, but among other factors of influence responsible for disease progression.[67]

For the establishment of polymer networks with defined mechanical properties, the length of the polymer chains between crosslinking units, degree of crosslinking, as well as the swelling properties, are important factors. Berg *et al.* showed that through variation of the chain length of PEG-urethane precursors, polymer networks with Young's modulus between 5 and 46 MPa can be generated. Owing to the hydrophilic nature of biopolymers, Young's modulus of the resulting networks was measured with 6–23 kPa.[28] In another study scaffolds were made of (D, L)-lactide-ε-caprolactone copolymers using different ratios of the monomer units. Results showed increasing Young's modulus with decreasing caprolactone (CL) content. In addition, the degradation properties were dependent on the monomer ratio.[68]

Having in mind the strategies and priorities described thus far a material platform with adjustable biomechanical and biochemical properties should be provided, which is applicable to a broader spectrum of TE applications. Following this challenge, a copolymer system with adjustable degradation properties, stiffness, and hydrophilicity was synthesized. Thus, our working group combined the properties of the highly degradable hydrophilic PLA and the slowly degradable hydrophobic poly-ε-caprolactone. Synthesis of (D,L)-lactide-ε-caprolactone methacrylate (LCM) copolymers was done by stannous catalyzed cationic ring opening polymerization of (D, L)-lactide and ε-caprolactone, followed by methacrylation of the hydroxyl-end groups of the polymer (Fig. 4A). Through variation of the molar ratio of lactide (LA) and CL, a material platform with defined biomechanical and degradation properties was established (Fig. 4B). Thus, when increasing the LA content the stiffness and hydrophilicity of the copolymer increased. Because of the high degree of ester bonds, LA-rich copolymers degrade faster than CL-rich copolymers. When decreasing the content of CL a more hydrophobic material with a slower degradation rate and lower elastic modulus can be established. Basic outlines of the preparation of LCM copolymers with defined biomechanical and biodegradation properties were already published.[69] Under all LCM variants two compositions were chosen; one as favored material for bone TE and the second composition for simulation of the tumor extracellular environment. The lactide-rich LCM_8:2, with a ratio of LA:CL of 8:2, is characterized by a high elastic modulus, and therefore suitable for bone reconstruction. In contrary, LCM_2:8 consists of a molar ratio of LA:CL of 2:8 and is much softer than the LCM_8:2 but degrades much slower. Obviously, this is advantageous for the simulation of the tumor ECM, for example, as an interesting approach in disease modeling. The degree of crosslinking was reduced to decrease the elastic modulus. Therefore, monomethacrylated LCM copolymers (LCMm) were synthesized using the same ratios of CL and LA as for the bifunctional ones (Fig. 4A). To reduce the elastic modulus of the pure LCM copolymers, bifunctional and monofunctional copolymers were mixed in defined ratios 100:0, 80:20, and 50:50 and crosslinked by ultraviolet (UV) curing (Fig. 4C). Elastic modulus was determined by relaxation experiments. The results show that the LA-rich polymer LCM_8:2 is stiffer (4.8 MPa) than the CL-rich copolymer LCM_2:8 (4.0 MPa). By reduction of the crosslinking degree from 100% to 50%, the mechanical strength decreased to 2.1 MPa for the LA-rich polymer and to 1.6 MPa for the CL-rich polymer (Fig. 5). It was demonstrated that through variation of LA and CL content or the degree of crosslinking a material platform could be established with adjustable mechanical properties. Thus, a higher amount of LA resulted in a more rigid crosslinked polymer, while by reducing the degree of crosslinking the stiffness of the polymer can be dramatically decreased.

It is of value to point out that the viscoelastic properties of the synthesized polymers are necessarily quite different from the stiffness of the porous scaffold, which is basically defined by the resulting scaffold structure and porosity. Due to the expected difficulties in determining the stiffness of a photochemically fabricated scaffold experimentally, a finite element analysis (FEA) was performed to calculate the stiffness of the structured 3D scaffolds. The numerical

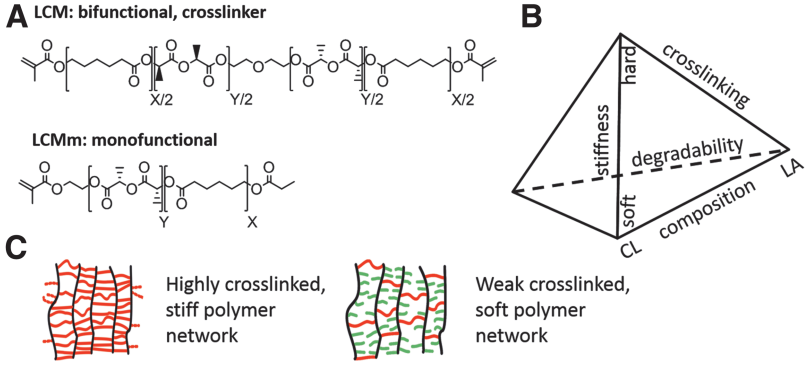


**FIG. 4.** Overview of the LCM polymer system: **(A)** bifunctional and monofunctional polyester LCM, **(B)** dependency of chemical composition on the biomechanical properties of the LCM copolymers, **(C)** illustration of stiff and soft network.

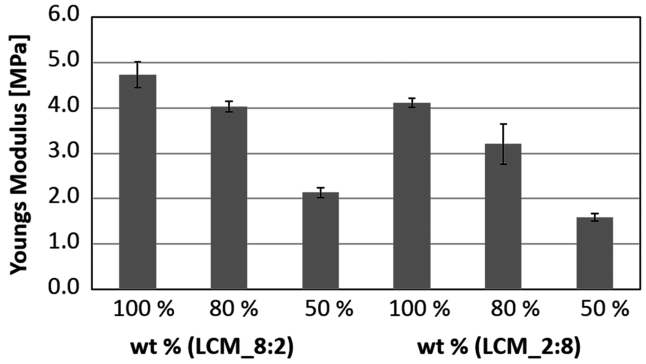


**FIG. 5.** Young's modulus of lactide- and caprolactone-rich copolymers with different crosslinking degrees.

results shown in Table 1 show exemplarily that the stiffness of a Schwarz P scaffold with $8\times8\times3$ unit cells is $\sim60$ times lower than the material stiffness given by the elastic or viscoelastic constitutive equation of the investigated polymer sample.

It is worth noting that the stiffness of osteoid and cartilage lies between 10 and 50 kPa.[66] Therefore, mechanical properties of LCM_8:2 scaffolds are in the correct range for bone and cartilage reconstruction. In comparison with that, stiffness of LCM_2:8 scaffolds is moderately reduced according to our expectations and met the observed range of tumor tissue (1–100 kPa). Evidently, the stiffness of a scaffold can be reduced further when using other unit cells, like cubic or woodpile structures.

### *Surface coating techniques*

Biomaterials and scaffolds made thereof interact with biological systems among others through their surfaces. Therefore, it is extremely important to control the surface properties and the functionality of a scaffold to recreate at least partially the conditions of the natural ECM. Organic thin films and coatings, particularly those of natural ECM constituents, are very attractive as biomaterial coatings because they offer great versatility to modulate and to control cell behavior.

It is well known that scaffolds made of synthetic polymers are usually characterized by a lack of cell adhesion sequences, which results in poor cell attachment and cell proliferation. Therefore, scaffolds for TE are usually coated with bioactive molecules to improve cell adhesion properties. There exist a huge number of different surface coating strategies, which can roughly be divided into covalent and ionic/electrostatic modification techniques. For electrostatic coating procedures one needs polycations such as poly-L-lysine and polyanions such as glycosaminoglycans to generate a so-called polyelectrolyte multilayer (PEM),[70] employing common LbL techniques. Usually the first layer is the polycation, followed by more or less washing steps and the subsequent coating of the sample with the selected polyanion to build up the typical bilayer structure. This procedure is repeated until the needed layer thicknesses are generated. Intensive investigations published by the authors of this study have shown that the LbL technique possesses a tremendous potential for surface coating of complex biomaterial structures like scaffolds. In brief, PEMs with poly-L-lysin (PLL) as polycation and heparin or chondroitin sulfate as polyanion were investigated, and the results showed an enhanced cell proliferation when increasing the stiffness of the PEM by treatment of the PEM with glutamic acid, which directs chondroitin sulfate from random coil structure in the stiffer intermolecular beta-sheet.[70] In detail this means that (1) the conformation state of the protein backbone and (2) the layer stiffness can be controlled precisely to build up ECM analog coatings. In a study of Morand *et al.* PEMs based on PLL and poly-L-glutamic acid (PGA) were used to study the effect of α-melanocyte-stimulating (MSH) hormone on the proliferation of epithelia cells and fibroblasts. Covalently coupled MSH-PGA showed a modulating effect on cell proliferation and the immune response.[71] Mehr *et al.* showed significant increase in mesenchymal stem cell proliferation and enhanced mineral formation on PLL-chitosan coated PCL-cylinders.[72] Gai *et al.* presented a theoretical method for contact printing of PEMs with the background to reduce preparation time from several hours to 30 min.[73] Sailer *et al.* established PEMs with stiffness gradient using poly(allyl amine) hydrochloride and poly(acrylic acid). HEK293 cells and embryonic rat spinal commissural neurons preferred intermediate modulus.[74] Interested readers are requested to get closer information about this approach from an excellent textbook recently published by C. Picart *et al.*[75]

Despite the fact that scaffolds based on triply periodic minimal surface (TPMS) structures should provide optimal fluid mechanical conditions for the reproducible establishment of LbL coatings, numerous biomolecules such as collagen provide not sufficient charge excess to generate a stable balance between intrinsic and extrinsic charge compensation.[76,77]

Therefore, an alternative option is given by coating techniques involving chemical grafting onto biomaterial surfaces. An interesting strategy to introduce a cell responsive surface is to covalently attach biomolecules or cell adhesion sequences to the surface of a scaffold using heterobifunctional linker molecules such as sulfo-SANPAH (N-succinimidyl-6-(4′-azido-2′-nitrophenylamino)-hexanoate). The coating procedure occurs in a two-step chemical reaction. First, N-succinimide functionality of the linker is allowed to react with the amine of the biomolecule forming an amide bond. After that, UV-triggered insertion reaction leads to covalent attachment of activated biomolecule in the aliphatic backbone of the polymer. Using this linker molecule adhesion sequences such as RGD-peptide[78,79] or fibrinogen fragments[80] were already successfully bound to polymer surfaces leading to an increase in cell attachment and proliferation. Nishitani *et al.* showed that covalent attachment of fibrinogen using sulfo-SANPAH crosslinking

Table 1. Numerical Stiffness Values of an $8\times8\times3$ Schwarz P Scaffold Estimated by Finite Element Analysis

| *LCM_8:2 in %* | *Young's modulus in kPa* | *LCM_2:8 in %* | *Young's modulus in kPa* |
|---|---|---|---|
| 100 | 74–78 | 100 | 67–70 |
| 80 | 65–69 | 80 | 46–61 |
| 50 | 34–37 | 50 | 25–28 |

leads to increased cell adhesion and calcium deposition.[81] In another study of Yip *et al.*, collagen was coupled to polyacrylamide gels with stiffness gradient reaching from 6 to 110 kPa. Enhancement of intracellular traction stress was determined on stiffer substrates.[82]

A protocol for the photoinduced covalent coating of collagen, the main component in ECM, was established. The evidence of the successful coating was provided by atomic force microscopy (AFM) phase-shift imaging. AFM phase-shift imaging is a useful tool to contrast material or mechanical changes on a surface with minor topographical features.[83] In comparison (Fig. 6) the mean phase shift of uncoated disks (upper images) is obviously lower than that on coated disks (lower images) due to the successful attachment of collagen. In detail, fibrillar collagen structures are formed, resulting in larger phase-shift amounts. This indicated that collagen is covalently bound to the polymer surfaces. In the next step, LCM_8:2 and LCM_2:8 scaffolds ($8\times8\times3$ Schwarz P unit cells) were labeled with collagen Type I. To quantify the amount of collagen inside the scaffold, the biomolecule was labeled with Sirius red, followed by the removal of bound Sirius red according to a protocol published by Sittichokechaiwut *et al.*[84] The absorbance of Sirius red was measured using a microplate reader, and the bound collagen was calculated with a standard curve of Sirius red-stained collagen. The results in Figure 7 demonstrate that 0.28–0.35 $\mu g/mm^3$ collagen was bound successfully inside the scaffold material.

## Methods Used for Scaffold Production

It is widely accepted that an ideal scaffold should consist of a 3D structure that should favor not only cell attachment and growth but also their further organization and possibly differentiation into functional tissue. In the context of these ambitious objectives, general requirements to end up with an ''ideal scaffold'' can be summarized as follows[85]:

1. Architecture:

Scaffolds should provide an open porous structure for vascularization, cell ingrowth, and new tissue formation. The scaffold structure must allow an efficient nutrient and metabolite transport, and degradation kinetic upon implantation should match the rate of new tissue formation and stiffness increase.

2. Cyto- and tissue compatibility:

Scaffolds should provide a suitable environment for cell attachment, proliferation, and differentiation under *in vitro* and *in vivo* conditions (biocompatibility).

3. Bioactivity:

Scaffolds should allow an active interaction with the cellular components of the engineered tissues to facilitate and regulate their activities. Consequently, the employed biomaterials may provide biological cues such as cell-adhesive ligands and peptides for protease-based matrix degradation or physical cues such as a hierarchically structured topography and morphology to influence cell phenotype and alignment.

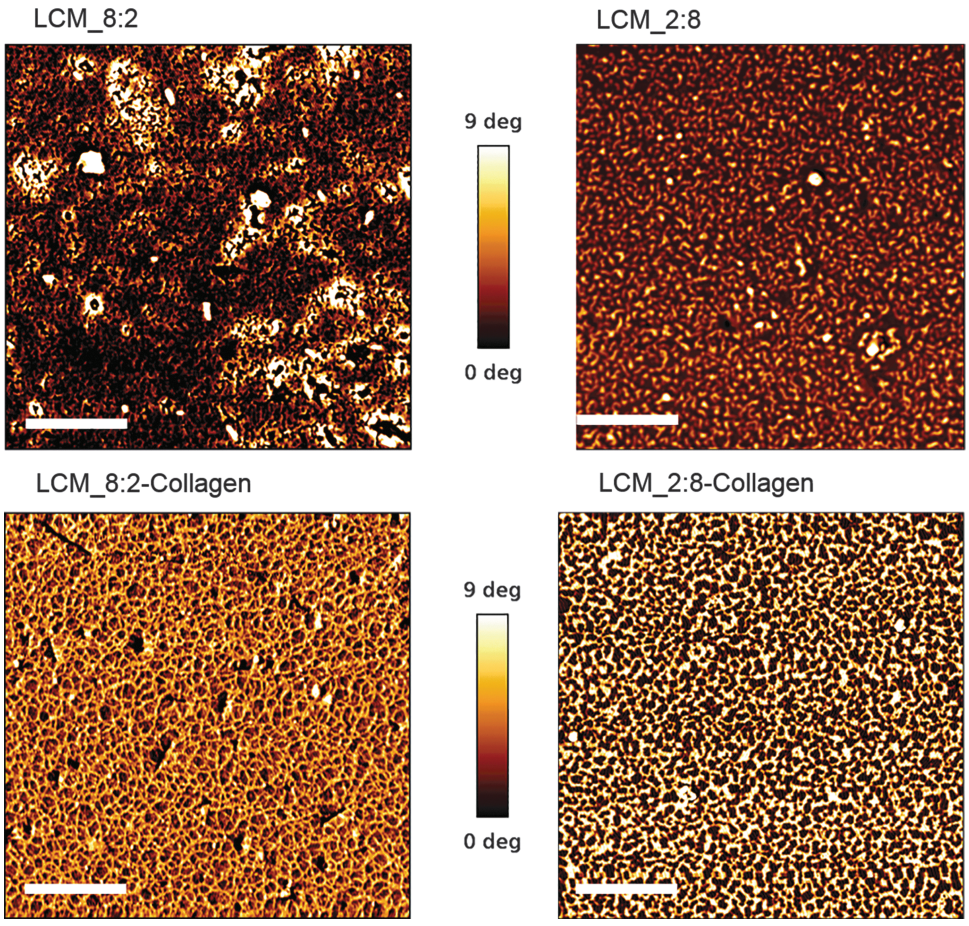


**FIG. 6.** Biofunctionalization of LCM samples with collagen Type I and characterization by atomic force microscopy (scale bar 500 nm).

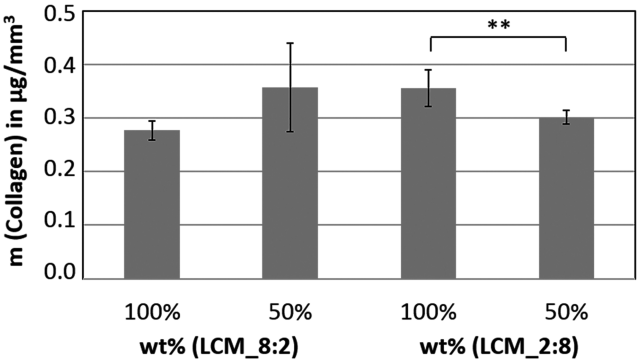


**FIG. 7.** Quantification of the surface-bound collagen Type I in LCM_8:2 and LCM_2:8 scaffolds using Sirius red staining (*t*-test: $^{**}p < 0.01$).

4. Drug delivery:

The used biomaterials and/or scaffolds made thereof may serve as a drug delivery system or reservoir for exogenous growth-stimulating signals such as growth factors to speed up regeneration pathways or antimicrobial substances to avoid biomaterial-associated infections in case of therapeutic treatments.

5. Mechanical properties:

Scaffolds provide mechanical shape and stability similar to the site-specific natural ECM. Recent studies on mechanobiology and mechanosensing have highlighted the importance of the mechanical environment of the seeded cells on the macro-, micro-, and nanoscale for regenerative and disease-modeling purposes.

The advent of the nanobiomedicine era can be dated back to the early 2000 years. Since this time an ever-increasing number of researchers tried to produce cell culture substrates or implantable devices with morphologies in the nanometer range.[86] In the last three decades several methods were established for the preparation of scaffolds (Fig. 8), such as solvent casting,[87] emulsion templating,[88] particulate leaching,[89] gas foaming,[90] electrospinning,[91] phase separation,[92] and freeze drying.[19] The limiting factor of these conventional methods was that the resulting 3D matrices are characterized by undefined pore sizes and geometries as well as an irregular spatial distribution of the pores. There was also a lack of pore interconnectivity observed within these 3D architectures leading to hindered transport of nutrients and metabolites inside the scaffold.[19,32] In light of the evidence that natural tissues show a hierarchical structure in association with an extreme complexity the development of artificial cell niches with a controlled heterogeneity seems to be of pivotal importance. From this key feature followed a tremendous need of techniques, which allow the controllable, reproducible, and site-specific fabrication of heterogeneous scaffolds. Over the years it became clear that additive manufacturing techniques possess this potential with different process-specific manifestations.

Innovative methods were established for generating scaffolds with defined pore sizes and pore distributions, such as fused deposition modeling,[93] selective laser sintering,[94] stereolithography (SLA),[95] and 2-PP.[96] These so-called RP techniques are manufacturing techniques in which 3D structures are generated in a LbL manufacturing process. RP techniques are based on computer-aided design (CAD) information, which is converted to a standard tesselation language (STL)-data format derived from the designation SLA. The model is converted into 2D layers incrementally stacked on top of one another to create a 3D structure.[19] The term SLA was first used in 1986 by C.W. Hull in his patent ''Apparatus for Production of Three-Dimensional Objects by Stereolithography.'' It is defined as a method and an apparatus for creating solid objects by successively ''printing'' thin layers of a photochemical reactive polymer on top of one another.[97]

In detail, in SLA free radical molecules are released upon interaction of photoinitiator molecules with UV light. Polymerization occurs up to a certain distance below the surface according to the possible penetration depth of UV light. After a given layer is selectively solidified, the structure

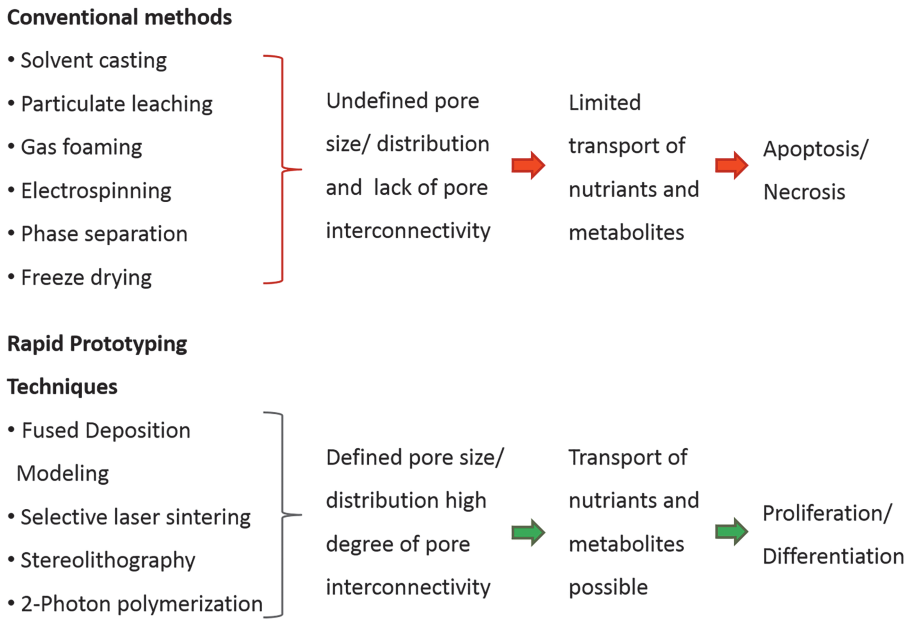


**FIG. 8.** Overview of the existing scaffold fabrication techniques.

is submerged within the photoresist by a depth that is equivalent to the thickness of the polymerized layer. Then the structure is recoated with fresh photoresist to enable processing of the next layer. After fabrication of the desired 3D structure, it is placed into an appropriate solvent to remove the nonpolymerized photoresist.[98] The versatility in design and precise nature of SLA enable fabrication of complex scaffolds with physiologically relevant microstructures. Scaffolds with well-defined pore sizes, porosities, pore distributions, pore interconnectivity, and pore gradients have already been fabricated using SLA.[26] Nevertheless, the UV light exhibits a depth of penetration that exceeds the layer thickness, resulting in overcuring of the previously solidified material and adhesion between the layers.[98] However, an essential drawback is the missing ability to generate structural features across multiple length scales (nm–cm) referring to the hierarchical structure of natural human tissues.[99]

From this point of view it is worth mentioning that 2-PP enables the generation of 3D structures with an extreme high resolution.[100] This method represents a maskless photolithographic technique, which enables 3D direct laser writing of various photoresists.[31] In 2-PP simultaneous absorption of two photons creates a virtual state for several femtoseconds. When a specific photoinitiator that reacts at a wavelength of 400 nm simultaneously absorbs two photons at 800 nm wavelength, their energy equals the energy of one photon at 400 nm, thus initiating a polymerization process (Fig. 9A). Photopolymerization triggered by nonlinear excitation occurs only in the focal point (voxel volume), without affecting other nearby regions.[25,100] Ultrafast infrared lasers with femtosecond pulses are used to generate the energy, which is needed for the 2-photon process. To achieve the tight focusing conditions required for multiphoton polymerization, conventional microscope objectives are used. The laser beam is focused through an objective into an infrared transparent sample to initiate 2-photon absorption. By moving the laser focus inside the photosensitive resist, a 3D structure can be generated[98] (Fig. 9B). During the polymerization process, either the photopolymer is moved to a fixed focal point or the focal point is moved within the photocurable sample. Movement of the laser beam is commonly accomplished using galvanomirrors, which scan the beam in the X- and Y-directions, and a piezoelectric stage, which moves the photopolymer in the Z-direction.[97,98] Either using a fast mechanical shutter or an acousto-optic modulator can achieve beam control, while beam intensity control can be achieved using neutral density filters, a variable attenuator or a combination of a polarizer and a wave plate.[97] After completion of the photopolymerization process, the nonphotopolymerized resin is removed, and the samples are developed in an appropriate solvent similar to any other lithographic process.[97] It should be mentioned that the above-described reaction conditions must be compatible with cell biology. 2-PP provides several advantages over conventional processes for scalable fabrication of components. Many materials processed by 2-PP are widely available and are inexpensive. In addition, numerous materials are transparent to near-infrared light.[98] Despite the light exposure constraints, 2-PP allows the fabrication of heterogeneous custom-made scaffolds according to the above-formulated requirements.

In the last decade, numerous commercial 2-PP systems were launched in the market. Exemplarily Nanoscribe GmbH (Germany), Multiphoton Optics GmbH (Germany), or FEMTIKA (Lithuania) operate on the market. Currently described investigations were performed using a 2-PP demonstrator system developed by avatera*medical* Mechatronics GmbH (Germany). The established system possesses a traversing range of $140 \times 50 \times 100\,mm^3$ (x, y, z), a position resolution of $\sim 100$ nm in x–y and a precise reproducibility of 200 nm. Because of these specifications, scaffold preparation performed by this 2-PP system showed an excellent reproducibility and relatively low geometrical errors when comparing the STL-data with the final structure (1–2%). The user can work with the system over HMI (Human Machine Interface) connected through LAN (Local Area Network). This system was further optimized to become an industrial 2-PP unit, which is characterized by a velocity up to 500 mm/s, a resolution of 2.5 nm, and a movement area of $200 \times 200\,mm^2$ (Fig. 10A/B).

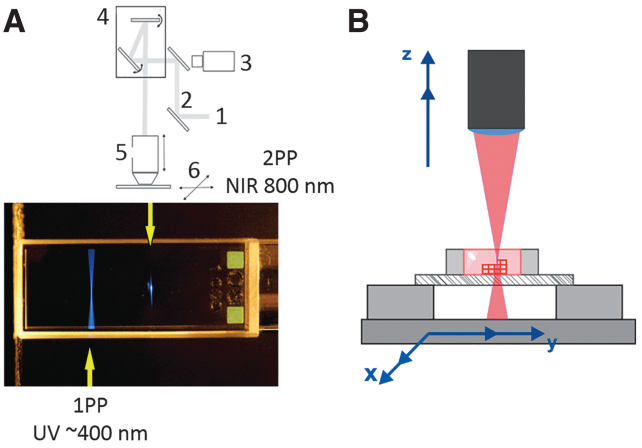


**FIG. 9.** **(A)** Comparison of the focal point of 1-photon absorption and 2-photon absorption (1: Ti-Sa-laser; 2: mirrors; 3: CCD camera; 4: galvano scanner; 5: objective lens; 6: mobile stages), **(B)** scheme of 2-PP of three-dimensional structures. 2-PP, two-photon polymerization.

### Designer Scaffolds Based on TPMSs

Cellular solids, which include regularly repeating lattice structures, have already been investigated in biomedical engineering and implantology where their controllable stiffness and porosity enable a reduction of stress shielding of load bearing implants.[101] In regenerative medicine and TE an advanced scaffold design requires (1) an optimal compromise between mechanical stiffness, transport properties, or permeability associated with its pores,[102] and (2) structural and functional biomimicry with the natural blueprint the structural hierarchy of the native tissue. For that reason, scaffolds with site-specific stiffness over multiple length scales provide the optimal mechanical strength and can be considered as bioinspired from a mechanical point of view. In addition to the mechanical behavior, the fluid permeability should allow superior diffusion to facilitate nutrient and metabolic waste transport. Moreover, a large surface area facilitates an optimal cell attachment, whereas a large pore volume enables the accommodation of the necessary cell mass for tissue genesis or regeneration.[103–105]

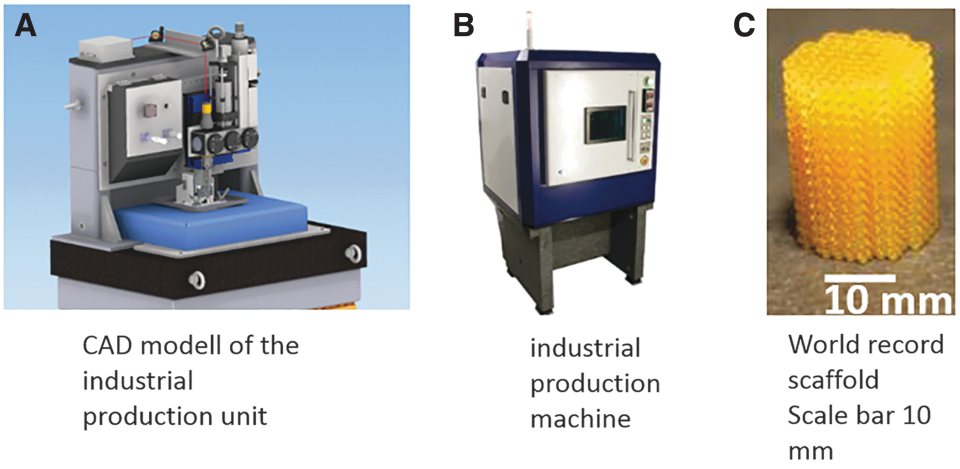


**FIG. 10.** **(A)** CAD model of industrial production unit, **(B)** industrial production machine, and **(C)** macroscale scaffold in the centimeter range made of LCM. CAD, computer-aided design.

Recently published studies provide evidence that pore diameter and nanotopography may affect proliferation and migration of different cell types.[106–108]

TPMSs in general and Schwarz P surfaces in particular offer the ability to tailor-made a suitable pore size, high surface-to-volume ratio, sufficient porosity, and high pore interconnectivity, respectively. The relevant RP fabrication process is completely software controlled, and therewith reproducible and scalable with a high degree of freedom. The establishment of ''designer scaffolds'' has become a feasible option, including an in-depth knowledge of the corresponding structure–property relationships.

Triple periodicity means that a minimal surface is periodic in three distinct Cartesian directions. TPMSs exist in nature in liquid crystals, zeolites, soluble protein, in lipid–protein water phases or in cell membranes.[109] The most common and popular TPMS structures in TE are, for example, Schwarz primitive (P), the Schwarz diamond (D), or the Schoen gyroid (G) minimal surfaces (Fig. 11). Scaffolds fabricated by 2-PP are made up by arranging unit cells next to each other using a CAD. The resulting bicontinuous scaffolds are characterized by a high interconnectivity and high porosity. TPMSs are smooth infinite surfaces that divide the whole domain of a unit cell into two intertwining and unconnected subdomains.[109,110] Cell seeding protocols and dynamic cultivation protocols are often derived from perfusion experiments where the wall shear stress caused by media flow is one of the dominant factors that influence initial cell adhesion. FEA led to the conclusion that Schwarz P surfaces provide the largest fluid permeability among all of the other triply periodic surfaces combined with the lowest shear stress level (Fig. 11).

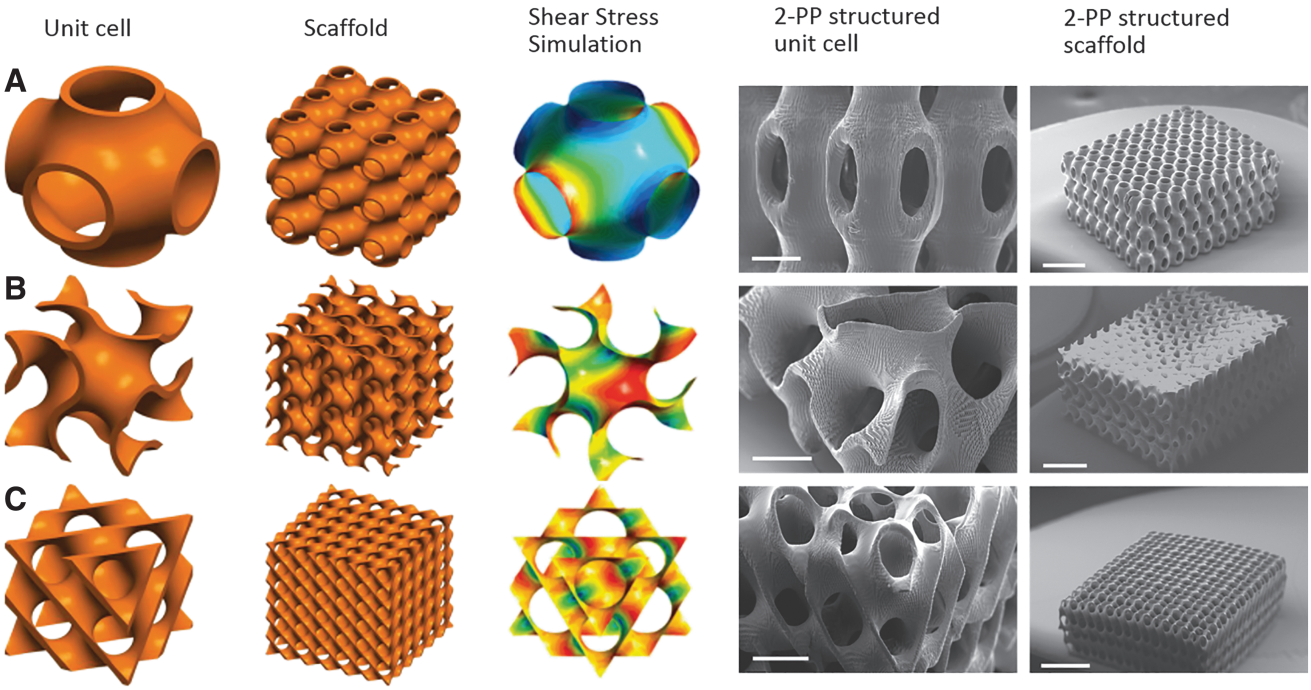


**FIG. 11.** CAD model of unit cell, scaffold and shear stress simulation, and SEM images (scale bar *left* image 200 µmn *right* image 1 mm) of 2-PP polymerized unit cell and scaffold of **(A)** Schwarz P, **(B)** Gyroid, and **(C)** Diamond triply periodic minimal surface. SEM, scanning electron microscopy.

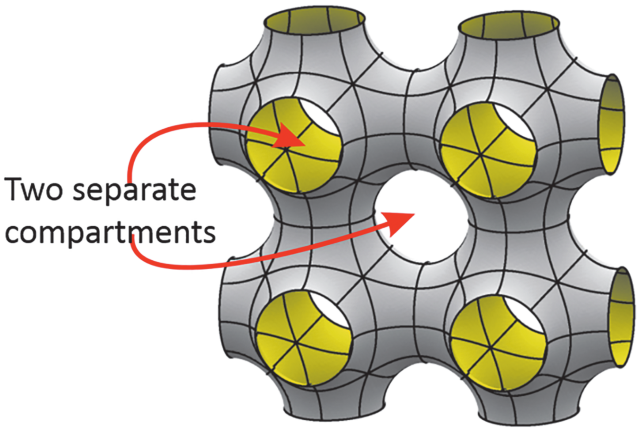


**FIG. 12.** Illustration of the two compartments of a scaffold made up of Schwarz P unit cells.

Scanning electron microscopy (SEM) images from 2-PP-fabricated scaffolds based on TPMS are shown in Figure 11, including the photochemical implementation of the preset geometry of the microstructure into a final scaffold structure. As mentioned above TPMS-based structures partition the available space into two intertwining compartments, and therefore offer completely new options for cell cultivation and tissue regeneration (Fig. 12). On the one hand, two cultivation compartments can be used in parallel, or on the other hand separated from each other for example to introduce cocultivation regimes based on two cell types, or alternatively one cultivation compartment and one media supply compartment.

On that background it should be mentioned that 2-PP processing allows in principle the implementation of a defined permeability between the two compartments by a suitable setting of the scanner velocity, hatching, and slicing parameters. Thus more or less porous walls can be generated (Fig. 13), leading to a customized diffusion ability of nutrients, metabolites, or cytokines between the compartments. In the last decade, various experimental setups for cell seeding and cell cultivation in the field of TE were introduced. Traditional static cell culture systems such as multiwell plates or Petri dishes ignore the fact that usually a dynamic environment *in vivo* surrounds cells. Obviously, limitations of conventional cell culture methods are mainly diffusion-based gradients of nutrients, metabolites, or cell masses leading to a decrease in cell stimulation. Therefore, different dynamic culture systems such as stirred or rotating wall vessel bioreactors and perfusion bioreactors were established.[111] When using wall vessel bioreactors stirring occurs only outside of the scaffold that a complete perfusion of the scaffold is improbable. Perfusion bioreactors are advantageous alternatives for cell seeding and cell culture since the whole scaffold structure is exposed to a forced and controlled flow-through. In this manner an optimal supply with nutrients can be achieved across the cross-section of the scaffold.[112] While static cell culture methods show inhomogeneous cell distribution and nutrient levels, cell seeding using perfusion bioreactors resulted in an increase of cell number and a more homogeneous cell distribution.[113] In Figure 14, a perfusion chamber (A) and the whole perfusion cell culture system (B) are shown. In the ever-increasing field of bone TE the effect of shear stress on the differentiation of cells can play a key role. Thus, it was shown that shear stress can lead to the activation of mechanotransductive signals and to expression of bone tissue matrix proteins.[114] In other recently published studies it was found that parameters such as static pressure, flow rate, flow pulsation, temperature pH- and $pO_2$ value have an effect on cell proliferation and cell viability.[115] Anisi *et al.* analyzed the effect of shear stress on spreading of cells. Thus, a physiological flow velocity of 48 mL/min showed no influence on cell adhesion.[116] It was also demonstrated that cell response could be improved when seeding cells using perfusion bioreactors.[94]

Putting the individual pieces together like in a puzzle, a conceptual framework to establish custom-made or designer scaffolds comes up. Essential components for this are as follows: (1) an extremely flexible material platform consisting of (D,L)-lactide-ε-caprolactone (LCM) to tailor-made biomechanical and biochemical features, (2) suitable coating techniques to render the surface of the scaffold bioactive, (3) an additive manufacturing process based on the photolithographic 2-PP to enable a controllable and reproducible fabrication of heterogeneous scaffolds, and (4) the introduction of biomimetic minimal surface scaffold designs to take advantage of mathematically defined stiffness, porosity, and permeability. The entire design process is summarized in Figure 15, and constitutes the framework to study organ-specific regeneration and disease processes of various pathologies.

### Future Application in Bone TE

Bone defects, which occur from injuries or chronic illnesses such as osteoporosis or rheumatic arthritis, pose a

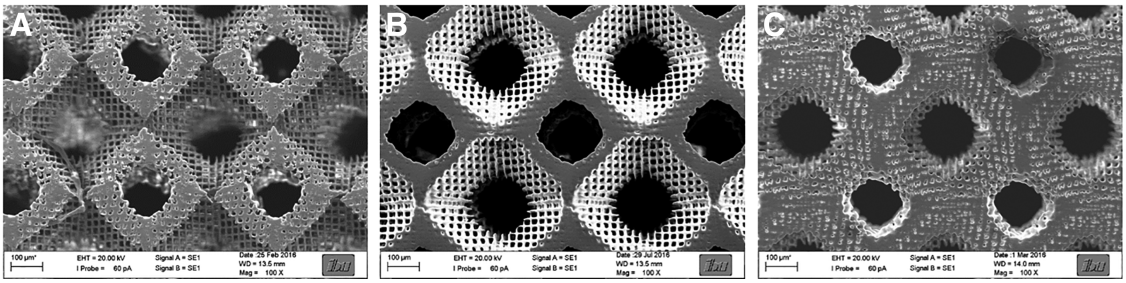


**FIG. 13.** Variation of galvano scanner velocity to generate Schwarz P scaffolds with porous diffusible walls: **(A)** 100 mm/s, **(B)** 90 mm/s, and **(C)** 80 mm/s.

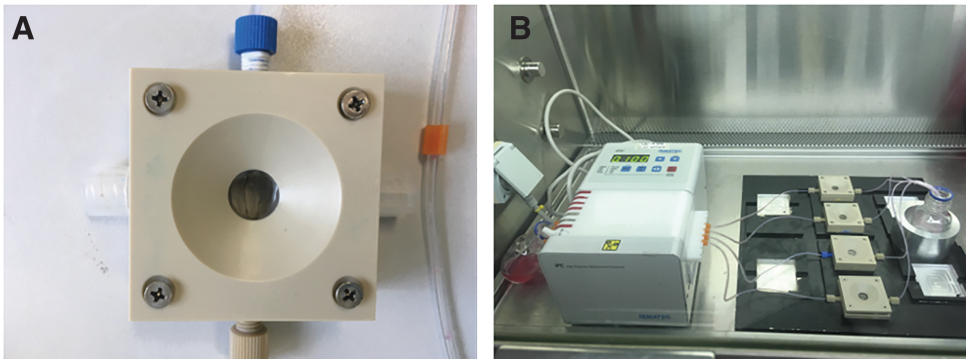


**FIG. 14.** Illustration of **(A)** perfusion chamber and **(B)** perfusion-cell-culturing system, equipped with peristaltic pump, four perfusion chambers, cell culture medium flask, and heating system.

huge challenge for current research activities. For the reconstruction of large bone defects, the material should possess biochemical, biophysical, and morphological properties such as biocompatibility, biodegradability, mechanical stability, high porosity, and interconnectivity. The degradation rate should be in an appropriate range, so that the implant can be replaced by naturally produced bone. Thus, several studies used biodegradable polyesters, such as PLA, PCL,[34] or Poly(lactide-co-glycolid) (PLGA),[38] to generate implants for bone regeneration. Especially copolymers, based on PCL and PLA, possess many advantages, such as adjustable degradation properties, stiffness, and a low amount of acid degradation products.

It seems obvious that the established material platform based on PLA-co-PCL copolymers with a LA:CL ratio of 8:2 should be a valuable option for bone TE applications. The stiffness of the material was further reduced by mixing dimethacrylated and monomethacrylated copolymers. The results for the LCM_8:2 polymer system are already shown in Figure 5.

To identify if the stiffness of the polymer network has an influence on the proliferation of preosteoblasts, proliferation studies were performed on 2D samples. Therefore, polymer disks were prepared by UV curing of mixtures of LCM_8:2 and LCMm_8:2 in ratios of 1:0 (100%), 0.8:0.2 (80%), and 0.5:0.5 (50%). Samples were coated with collagen I using the heterobifunctional crosslinker sulfo-SANPAH to ensure good cell adhesion, which is due to the cell adhesion sequences of the collagen, which promotes cell attachment, proliferation, and differentiation through receptor-mediated interactions.[117] Ovine mesenchymal stem cells (oMSCs) were seeded on the disks and cultured for 3 days. Then, proliferation of oMSCs was quantified by counting the trypsinated cells (Fig. 16). The results show an influence of the stiffness on the proliferation rate. Thus, on stiffer substrates proliferation was higher than on the softer materials. The observed results are in accordance with a recently published study of Yilgor *et al.*, showing that oMSCs proliferate faster on stiffer materials.[118]

After the 2D experiments, scaffolds were produced by 2-PP using three different ratios of LCM_8:2 and LCMm_8:2 and the Schwarz P minimal surface as unit cell. In brief, $8 \times 8 \times 3$ unit cells with a dimension of 520 µm were arranged to each other with an overlap of 20 µm and developed in acetone for 7 days. SEM images of scaffolds showed the successful generation of highly porous scaffolds with a high interconnectivity between the pores (Fig. 17). The scaffolds were likewise coated with collagen I using the heterobifunctional crosslinker sulfo-SANPAH to increase cell adhesion. We further quantified surface-bound collagen I using Sirius red staining. An amount of 0.28–0.35 µg/mm$^3$ collagen I was covalently attached to the scaffold. After sterilization of the scaffolds, they were fixed into perfusion chambers, seeded with oMSCs in accordance with an *ex ante* established protocol. Cells were cultured for 21 days under static conditions. After 7 days, the cell culture medium was

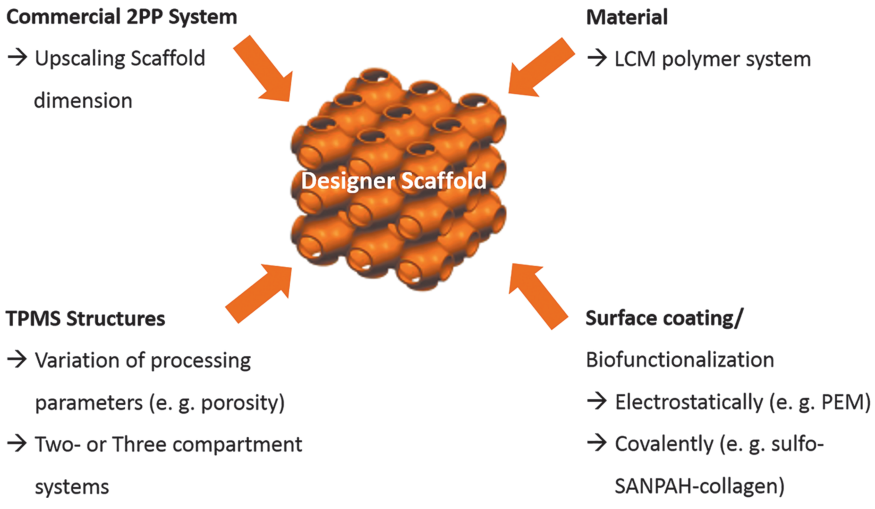


**FIG. 15.** Components of the conceptual framework to establish designer scaffolds.

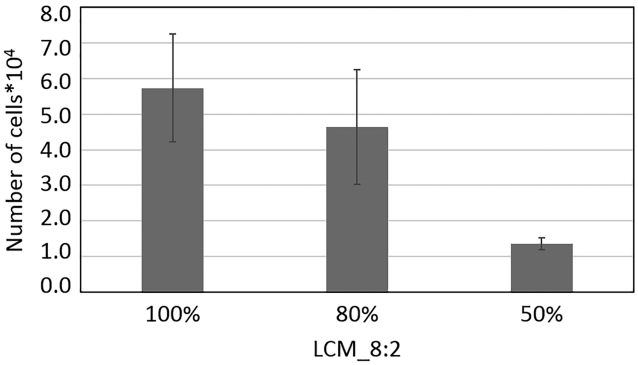


**FIG. 16.** Proliferation kinetics of oMSCs on collagen I-coated UV-cured LCM_8:2 100%, LCM_8:2 80%, and LCM_8:2 50% polymer disks. Cells were seeded on polymer disks and cultured in expansion for 3 days. oMSCs, ovine mesenchymal stem cells; UV, ultraviolet.

changed against differentiation medium. In Figure 18A time-dependent proliferation of oMSCs is shown. We observed an enhancement of the cell number with increasing cultivation time up to 230,000 cells after 3 weeks. This refers to a cell density of 7200 until 8500 cells per $mm^3$ after a cultivation time of 21 days. In contrast to the performed 2D experiments, no significant effect of the stiffness of the scaffold on the cell proliferation efficiency was observed. This is due to the fact that cells grow inside the porous scaffold structure in the third direction in which intercellular cell–cell interactions influence the proliferation much more than the stiffness of the material. This effect occurs already at early cultivation times (72 h), where locally 3D growth has been observed. To support this hypothesis, the actin filaments and the nucleus were stained for confocal fluorescence microscopy. In Figure 18B and C, the morphology of oMSCs cultured for 3 weeks within the LCM_8:2 scaffold is shown. Results demonstrate that oMSCs build up a confluent cell layer around the whole scaffold, and the magnification from inside the scaffold pores showed that cells proliferate in three directions to form a 3D cellular network. Thus, it can be hypothesized that the effect of stiffness on the overall cell response is slightly suppressed in comparison with the 2D results.

In a study of Raimondi *et al.* a correlation between pore size and cell–cell interaction was shown. They demonstrated a strong interaction between the MSCs inside scaffold pores with a diameter of 200 μm.[119] This result is in accordance with the observed proliferation of the oMSCs within the LCM scaffold. Another study by Marino *et al.* reported 3D proliferation of preosteoblasts in 2-PP-structured scaffolds. Also an increased osteogenesis in dependence of the 3D structure, biofunctionality, and Young's modulus was demonstrated.[18] We further examined the production of ECM by oMSCs using SEM and energy dispersive X-ray spectroscopy (EDX) analysis. SEM image inside a Schwarz P unit cell showed a confluent cell layer (Fig. 18D; upper part of the image) and cluster-like structures (arrows). According to EDX measurements, these aggregates showing a stoichiometric mass ratio equivalent to hydroxyl apatite (Fig. 18E). Remarkably, the oMSCs proliferate until the complete scaffold was filled and start to differentiate by inducing mineralization. It can be concluded that the conceptual framework developed so far can be successfully transferred to bone TE applications. The established material platform, based on LA and CL copolymers in combination with TPMS structures, has shown an excellent capacity for the fabrication of designer scaffolds for bone TE. The cultured oMSCs proliferate, differentiate, and start to synthesize their own mineralized ECM after a cultivation time of 3 weeks.

### Future Application in Tumor TE

The International Agency for Research on Cancer has estimated that the rates of global incidence as well as mortality associated with cancer will increase dramatically.

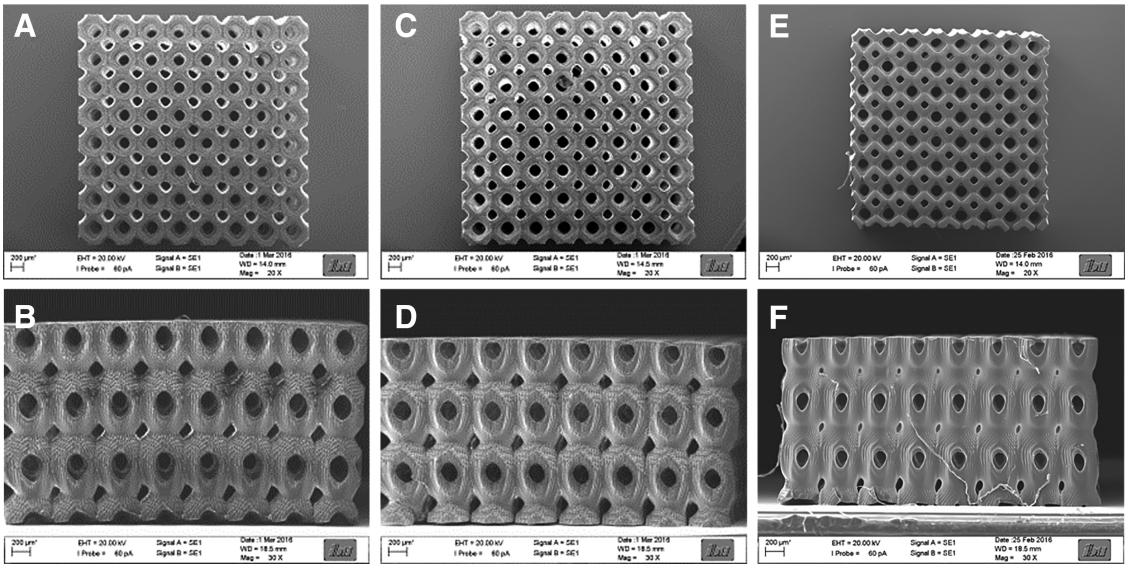


**FIG. 17.** SEM images of LCM_8:2 100% **(A, B)**, LCM_8:2 80% **(C, D),** and LCM_8:2 50% **(E, F)** scaffolds written by 2-PP with 8×8×3 Schwarz P unit cells (dimension: 520 μm; overlap 20 μm). The percentage value indicates the amount of bifunctional copolymer.

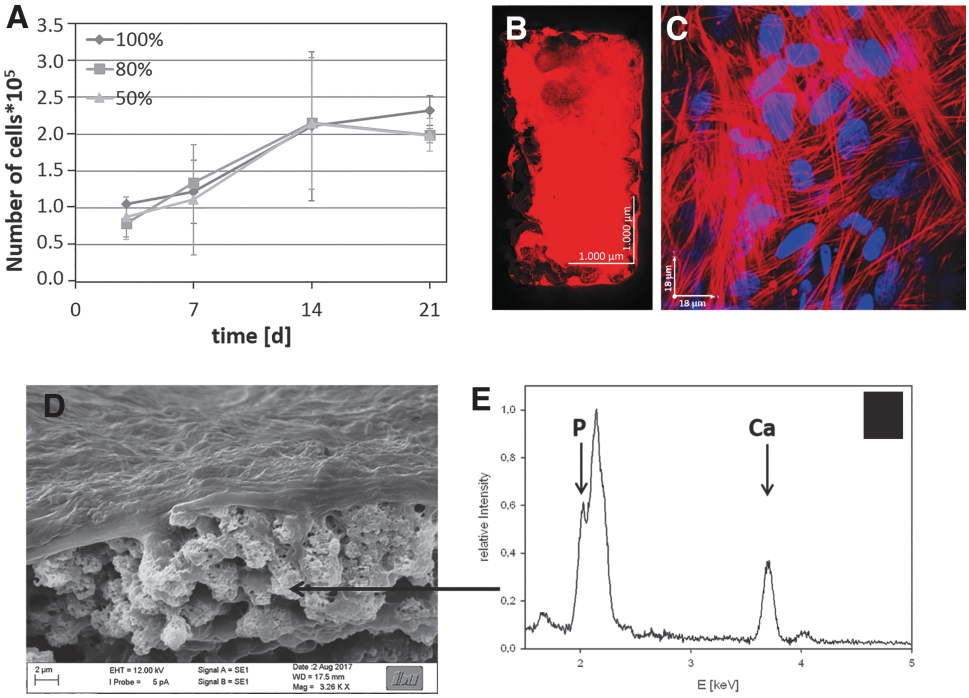


**FIG. 18.** Ovine MSCs were cultured on LCM_8:2 scaffolds of different stiffness for 7 days in normal cell culture medium and for additional 14 days in differentiation medium. **(A)** Time-dependent proliferation of oMSCs in LCM_8:2 100%, LCM_8:2 80%, and LCM_8:2 50% scaffolds; **(B)** confocal fluorescence image of a whole LCM_8:2 scaffold; and **(C)** magnification in the interior of unit cell of LCM_8:2 scaffold after culture time of 21 days (*red*: actin, *blue*: nucleus); **(D)** SEM image of LCM_8:2 scaffold cultured with MC3T3–E1 osteoblasts for 21 days; **(E)** EDX spectrum of calcified area inside the scaffold. EDX, energy dispersive X-ray spectroscopy.

It is expected that 27.5 million new cases and 16.3 million cancer deaths will be registered per year unitl 2040.[120] It is worth mentioning that metastases are responsible for ~90% of the mortality.[121] Despite great advances in basic and clinical research it is widely accepted that tumor progression and metastasis are strongly influenced by interactions between tumor cells and the cellular environment. It seems to be clear on this background that the research activities to establish an artificial 3D environment (ECM) for tumor cells have gained importance.[122,123]

The native ECM regulates adhesion, migration, and differentiation of cells through a highly dynamic up- and downregulation of growth factors, cytokines, or hormones.[124] In malignant neoplasms, this balance of chemical signal molecule regulation is disturbed. Moreover a stiffening of the ECM and a change in the contractile forces inside the cells through crosslinking between actin and myosin were observed.[125] Many studies have demonstrated that matrix stiffness correlates with tumor cell proliferation and differentiation. Thus, cells on a stiffer matrix upregulate Rho-GTPase, which leads to an increase in cellular contractibility. Furthermore, in a stiffer environment cells build up higher polymerized actin filaments. This leads as well to an increase in cellular stiffness.[21,126] As it was stated above culture platforms based on synthetic materials may be useful to overcome some limitations associated with natural or biological materials. However, several synthetic and natural polymers were introduced to investigate different aspects of tumor function such as PCL,[127] PLGA,[128] PEG,[129] or natural polymer matrices consisting of gelatin[130] or silk.[131] Due to its tunable physicochemical and biochemical properties, copolymers based on PCL were used to establish an artificial tumor microenvironment.[132]

Therefore, it appears reasonable to synthesize a CL-rich copolymer (LCM_2:8) based on LA and CL in a ratio of 2:8 with methacrylated end groups. To further reduce Young's modulus monomethacrylated CL-rich copolymers (LCMm_2:8) were synthesized using the same ratio of LA and CL as for the LCM_2:8 to ensure good comparability. Stiffness of the different polymer compositions is already shown in Figure 5. Bifunctionalized LCM_2:8 and monofunctionalized LCMm_2:8 were mixed in the ratios 1:0 (100%), 0.8:0.2 (80%), and 0.5:0.5 (50%) and UV cured to polymer disks to generate CL-rich networks with Young's modulus between 1.6 and 4 MPa. The effect of material stiffness on the proliferation of noninvasive Michigan Cancer Foundation 7 (MCF-7) cells was analyzed after a cultivation time of 3 days. In Figure 19, it is shown that the matrix stiffness had obviously an effect on the proliferation of the MCF-7 cells. Thus, proliferation increased with increasing polymer stiffness. It is well known that the mechanical properties of the ECM correlate with the invasive

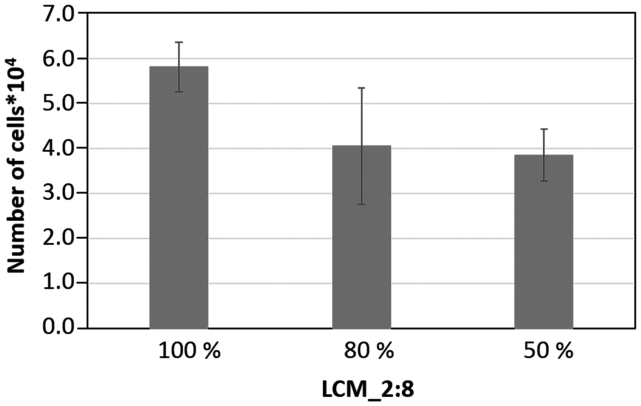


**FIG. 19.** Proliferation of MCF-7 cells on UV-cured and collagen I-coated LCM_2:8 100%, LCM_2:8 80%, and LCM_2:8 50% disks after 72 h of cultivation. MCF-7, Michigan Cancer Foundation 7 cells.

potential of tumor cells. Thus during tumorgenesis significant collagen deposition, linearization, and bundling lead to stiffening of the ECM, which leads to an increase of focal adhesions and other signaling pathways leading to a higher proliferation rate.[21,126]

After confirmation that tumor cells adhere and proliferate on CL-rich polymer disks, scaffolds of the three different ratios of LCM_2:8 and LCMm2:8 were produced by 2-PP using Schwarz P minimal surfaces. In brief, $8\times8\times3$ unit cells with a dimension of 520 µm were arranged to each other with an overlap of 20 µm and developed in acetone for 7 days. Because the LCM_2:8-scaffolds were significantly softer than the scaffolds polymerized with LCM_8:2, freeze drying during preparation for SEM led to massive shrinking processes. Therefore, morphology of the scaffold was characterized by confocal laser scanning microscopy (CLSM) (Fig. 20A–C). The images demonstrate a high interconnectivity of the scaffold pores as well as slight variations in the degree of crosslinking. As expected, scaffolds structured with only 50% crosslinker concentration showed a lower crosslinking degree. To render the scaffolds bioactive a coating with collagen Type I was carried out to ensure good mimicry of tumor microenvironment. Cell seeding with MCF-7 cells was performed using perfusion chambers. The proliferation was analyzed after static cell culture for 7, 14, and 21 days (Fig. 20D). Time-dependent proliferation showed an increase in cell number over the whole cultivation time for all materials with some differences in the proliferation rate. The cell density inside the scaffold was 33,600 until 40,200 cells per $mm^3$ after a cultivation period of 21 days.

The proliferation data did not significantly confirm the results in 2D where cell proliferation was higher on the stiffer substrates due to the nature of the 3D cell growth, where the cell–material contact becomes possibly less important. This phenomenon was also shown in another study, where cells showed different proliferation velocities in comparison with cells in a monolayer culture due to the cell–matrix and cell–cell interactions in scaffold-based cell culture systems.[131] Morphology of the tumor cells was characterized by CLSM. Therefore, tumor cell surface receptor CD44 and actin were labeled using appropriate antibodies. CD44 represents a cell surface receptor, which is upregulated in tumor cells and stimulates tumor cell proliferation, invasion, and migration.[133,134] In Figure 20E, the whole LCM_2:8 100% scaffold and in Figure 20F a detailed view of a Schwarz P unit cell are shown after 21 days of cultivation. It can be noticed that the entire LCM_2:8 100% scaffold is populated by the cells, and CD44 (green) is increasingly expressed by the cells. To sum up very briefly, it can be considered that the established material platform based on PLA-co-PCL copolymers with a LA:CL ratio of 2:8 showed a very good performance as artificial tumor environment.

It was demonstrated that noninvasive MCF-7 tumor cells proliferate better on stiffer 2D substrates. This tendency was clearly suppressed under 3D cultivation conditions since cell growth was observed in all three space directions until a confluent colonization appeared. Moreover, MCF-7 cells expressed tumor-specific cell surface protein CD44 and colonized the entire interior of the scaffold. Thus, it can be concluded that the strategy to combine a highly flexible polymer platform with a nanoscale 2-PP process based on TPMS surfaces and a superficial collagen Type I functionalization proved suitable for application in tumor TE.

## Conclusion

When creating scaffolds for TE application, the 3D constructs should have specific properties, such as biocompatibility, appropriate degradation rate, defined porosity, and interconnectivity, as well as site-specific mechanical properties. There exist a huge number of scaffold fabrication methods. Among these techniques, 2-PP enables the

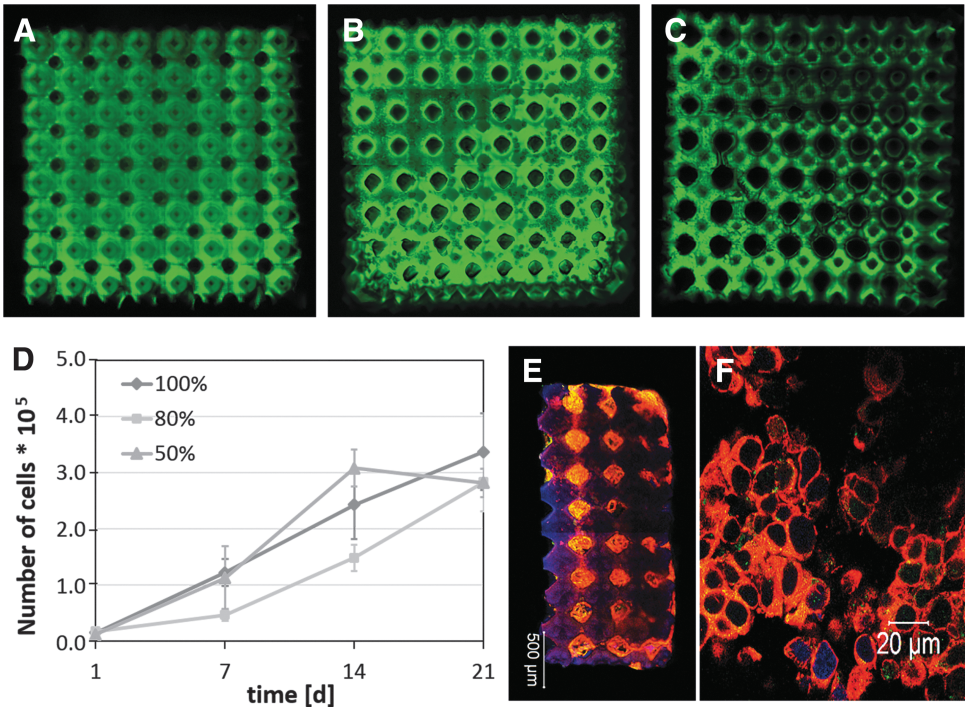


**FIG. 20.** Confocal fluorescence microscopy images of **(A)** LCM_2:8 100%, **(B)** LCM_2:8 80%, and **(C)** LCM_2:8 50% scaffolds written by 2-PP with $8\times8\times3$ Schwarz P unit cells (dimension: 520 µm; overlap 20 µm); MCF-7 cells were cultured on LCM_2:8 scaffolds of different stiffness for 21 days. **(D)** Proliferation kinetic of MCF-7 cells in LCM_2:8 100%, LCM_2:8 80%, and LCM_2:8 50% scaffolds; **(E)** confocal fluorescence image of a whole LCM_2:8 scaffold and **(F)** magnification inside one pore of LCM_2:8 scaffold after culture time of 21 days (*red*: actin, *green*: CD44, *blue*: nucleus). The percentage value indicates the amount of bifunctional copolymer.

fabrication of scaffolds with defined size and shape and a resolution in the nanometer range. In 2-PP unit cells are arranged to each other by moving the laser focus through a photoresist with nanoscale precision, whereas polymerization occurs only in the focus volume (femtoliter volume) leading to a nearly perfect control over the structure. Under the multitude of photocrosslinkable polymers, copolymers based on LA and CL showed distinct advantages that are mainly based on the adjustable mechanical and biodegradation properties.[69,135] Within our studies, we developed a material platform using different ratios of LA and CL to create copolymers, which can be used for bone TE as well as for tumor TE. Photochemical polymerization by 2-PP was performed using mathematically defined TPMS models, for example, Schwarz P minimal surfaces, so that the resulting scaffolds possess a controllable and exactly defined architecture, stiffness, porosity, and flow resistance. After biofunctionalization with collagen Type I, cell seeding was performed by perfusion bioreactors. First, cell studies demonstrated that both oMSCs and MCF7 cells proliferate in three dimensions and populate the whole scaffold. Furthermore, cell differentiation could be proven after 21 days of cultivation.

As outlined in the study a conceptual framework was introduced to fabricate custom-designed 3D scaffolds, named here as ''designer scaffolds'' for TE applications. The availability of an extremely flexible material platform based on PLA-co-PCL copolymers in combination with a nanoscale polymerization technique based on multiphoton absorption and software-based models, which allow the fabrication of scaffolds with perfectly controllable structure–property relations, provides new perspectives for diagnostic (disease-modeling) and therapeutic options (regenerative medicine) in the exciting field of TE.

Both application areas continue to move forward and take advantage of one another, thereby fostering the evolution of more advanced products. Fundamental challenges are summarized as follows:

- The next generation of organ-on-a-chip models in the field of disease modeling is based on bioinspired scaffold systems and able to provide a realistic physiological response, for example, to estimate the functional effects of drugs. Chip-based multiorgan models (body-on-a-chip, tissue interface-on-a-chip, parenchymal tissue-on-a-chip) enter the market having evolved well past the proof-of-concept stage.[136]
- The advent of induced pluripotent stem cells enables the transformation from human-on-a-chip models to person-on-a-chip models taking into consideration the genetic background of specific patients. Both regenerative approaches and disease models will profit from this exciting development with a remarkable speed.
- The development of custom-designed 3D scaffolds, named here as ''designer scaffolds,'' needs a technical platform, which allows a reproducible cell cultivation in the long term and a reliable monitoring of the cultivation process, including an unambiguous biomarker specification.[137]

In this regard the conceptual framework provided by this study represents an important piece of the entire puzzle and makes the process of scaffold fabrication more controllable in comparison with prevailing approaches.

## Acknowledgments

The financial support granted by the European Commission Research and Innovation DG (InnovaBone, Project No: 263363) and the ''Federal Ministry of Education and Research'' (DiaTumor, Project No: 13N12460) is gratefully acknowledged.

## Disclosure Statement

No competing financial interests exist.

## References

1. de Peppo, G.M., Thomsen, P., Karlsson, C., Strehl, R., Lindahl, A., and Hyllner, J. Human progenitor cells for bone engineering applications. Curr Mol Med **13,** 723, 2013.
2. Deplaine, H., Lebourg, M., Ripalda, P., *et al.* Biomimetic hydroxyapatite coating on pore walls improves osteointegration of poly(L-lactic acid) scaffolds. J Biomed Mater Res B **101b,** 173, 2013.
3. Lee, W.T., Koak, J.Y., Lim, Y.J., Kim, S.K., Kwon, H.B., and Kim, M.J. Stress shielding and fatigue limits of polyether-ether-ketone dental implants. J Biomed Mater Res B Appl Biomater **100,** 1044, 2012.
4. Schantz, J.T., Hutmacher, D.W., Lam, C.X.F., *et al.* Repair of calvarial defects with customised tissue-engineered bone grafts—II. Evaluation of cellular efficiency and efficacy in vivo. Tissue Eng **9,** S127, 2003.
5. Mandrycky, C., Phong, K., and Zheng, Y. Tissue engineering toward organ-specific regeneration and disease modeling. MRS Commun **7,** 332, 2017.
6. Xu, X., Farach-Carson, M.C., and Jia, X. Three-dimensional in vitro tumor models for cancer research and drug evaluation. Biotechnol Adv **32,** 1256, 2014.
7. Holzapfel, B.M., Reichert, J.C., chantz, J.T., *et al.* How smart do biomaterials need to be? A translational science and clinical point of view. Adv Drug Deliv Rev **65,** 581, 2013.
8. Lutolf, M.P., and Hubbell, J.A. Synthetic biomaterials as instructive extracellular microenvironments for morphogenesis in tissue engineering. Nat Biotechnol **23,** 47, 2005.
9. Schaefer, D., Martin, I., Jundt, G., *et al.* Tissue-engineered composites for the repair of large osteochondral defects. Arthritis Rheum **46,** 2524, 2002.
10. Wan, Y.Q., Feng, G., Shen, F.H., Laurencin, C.T., and Li, X.D. Biphasic scaffold for annulus fibrosus tissue regeneration. Biomaterials **29,** 643, 2008.
11. Schwarz, S., Koerber, L., Elsaesser, A.F., *et al.* Decellularized cartilage matrix as a novel biomatrix for cartilage tissue-engineering applications. Tissue Eng Part A **18,** 2195, 2012.
12. Santoro, M., Lamhamedi-Cherradi, S.E., Menegaz, B.A., Ludwig, J.A., and Mikos, A.G. Flow perfusion effects on three-dimensional culture and drug sensitivity of Ewing sarcoma. P Natl Acad Sci U S A **112,** 10304, 2015.
13. Barcus, C.E., Keely, P.J., Eliceiri, K.W., and Schuler, L.A. Stiff collagen matrices increase tumorigenic prolactin signaling in breast cancer cells. J Biol Chem **288,** 12722, 2013.
14. DeFail, A.J., Edington, H.D., Matthews, S., Lee, W.C.C., and Marra, K.G. Controlled release of bioactive doxorubicin from microspheres embedded within gelatin scaffolds. J Biomed Mater Res A **79a,** 954, 2006.
15. Breslin, S., and O'Driscoll, L. Three-dimensional cell culture: the missing link in drug discovery. Drug Discov Today **18,** 240, 2013.

16. Lovitt, C.J., Shelper, T.B., and Avery, V.M. Advanced cell culture techniques for cancer drug discovery. Biology (Basel) **3,** 345, 2014.
17. Provenzano, P.P., Eliceiri, K.W., Campbell, J.M., Inman, D.R., White, J.G., and Keely, P.J. Collagen reorganization at the tumor-stromal interface facilitates local invasion. BMC Med **4,** 1, 2006.
18. Marino, A., Filippeschi, C., Genchi, G.G., Mattoli, V., Mazzolai, B., and Ciofani, G. The Osteoprint: a bioinspired two-photon polymerized 3-D structure for the enhancement of bone-like cell differentiation. Acta Biomater **10,** 4304, 2014.
19. Peltola, S.M., Melchels, F.P.W., Grijpma, D.W., and Kellomaki, M. A review of rapid prototyping techniques for tissue engineering purposes. Ann Med **40,** 268, 2008.
20. Leventhal, A., Georges, P., and Janmey, P. Soft biological materials and their impact on cell function. Soft Matter **3,** 299, 2007.
21. Acerbi, I., Cassereau, L., Dean, I., *et al.* Human breast cancer invasion and aggression correlates with ECM stiffening and immune cell infiltration. Integr Biol-Uk **7,** 1120, 2015.
22. Cui, H., Webber, M.J., and Stupp, S.I. Self-assembly of peptide amphiphiles: from molecules to nanostructures to biomaterials. Biopolymers **94,** 1, 2010.
23. Thavornyutikarn, B., Chantarapanich, N., Sitthiseripratip, K., Thouas, G.A., and Chen, Q. Bone tissue engineering scaffolding: computer-aided scaffolding techniques. Prog Biomater **3,** 61, 2014.
24. Moroni, L., Nandakumar, A., Barrere-de Groot, F., van Blitterswijk, C.A., and Habibovic, P. Plug and play: combining materials and technologies to improve bone regenerative strategies. J Tissue Eng Regen M **9,** 745, 2015.
25. Liska, R., Schuster, M., Infuhr, R., *et al.* Photopolymers for rapid prototyping. J Coat Technol Res **4,** 505, 2007.
26. Skoog, S.A., Goering, P.L., and Narayan, R.J. Stereolithography in tissue engineering. J Mater Sci-Mater M **25,** 845, 2014.
27. Melissinaki, V., Gill, A.A., Ortega, I., *et al.* Direct laser writing of 3D scaffolds for neural tissue engineering applications. Biofabrication **3,** 1, 2011.
28. Berg, A., Wyrwa, R., Weisser, J., *et al.* Synthesis of photopolymerizable hydrophilic macromers and evaluation of their applicability as reactive resin components for the fabrication of three-dimensionally structured hydrogel matrices by 2-photon-polymerization. Adv Eng Mater **13,** B274, 2011.
29. Kufelt, O., El-Tamer, A., Sehring, C., Schlie-Wolter, S., and Chichkov, B.N. Hyaluronic acid based materials for scaffolding via two-photon polymerization. Biomacromolecules **15,** 650, 2014.
30. Ovsianikov, A., Deiwick, A., Van Vlierberghe, S., *et al.* Laser fabrication of three-dimensional CAD scaffolds from photosensitive gelatin for applications in tissue engineering. Biomacromolecules **12,** 851, 2011.
31. Marino, A., Filippeschi, C., Mattoli, V., Mazzolai, B., and Ciofani, G. Biomimicry at the nanoscale: current research and perspectives of two-photon polymerization. Nanoscale **7,** 2841, 2015.
32. Kapyla, E., Aydogan, D.B., Virjula, S., *et al.* Direct laser writing and geometrical analysis of scaffolds with designed pore architecture for three-dimensional cell culturing. J Micromech Microeng **22,** 1, 2012.
33. Melchels, F.P.W., Bertoldi, K., Gabbrielli, R., Velders, A.H., Feijen, J., and Grijpma, D.W. Mathematically defined tissue engineering scaffold architectures prepared by stereolithography. Biomaterials **31,** 6909, 2010.
34. Park, J.E., and Todo, M. Development and characterization of reinforced poly(L-lactide) scaffolds for bone tissue engineering. J Mater Sci-Mater M **22,** 1171, 2011.
35. Woodruff, M.A., and Hutmacher, D.W. The return of a forgotten polymer-Polycaprolactone in the 21st century. Prog Polym Sci **35,** 1217, 2010.
36. Park, S.H., Park, D.S., Shin, J.W., Kang, Y.G., Kim, H.K., and Yoon, T.R. Scaffolds for bone tissue engineering fabricated from two different materials by the rapid prototyping technique: PCL versus PLGA. J Mater Sci Mater Med **23,** 2671, 2012.
37. Perron, J.K., Naguib, H.E., Daka, J., and Chawla, A. A parametric study on the processing parameters and properties of a porous poly(DL-lactide-co-glycolide) acid 85/15 Bioscaffolds. Polym Eng Sci **49,** 2062, 2009.
38. Sander, E.A., Alb, A.M., Nauman, E.A., Reed, W.F., and Dee, K.C. Solvent effects on the microstructure and properties of 75/25 poly(D,L-lactide-co-glycolide) tissue scaffolds. J Biomed Mater Res A **70a,** 506, 2004.
39. Ovsianikov, A., Gruene, M., Pflaum, M., *et al.* Laser printing of cells into 3D scaffolds. Biofabrication **2,** 1, 2010.
40. Ovsianikov, A., Malinauskas, M., Schlie, S., *et al.* Three-dimensional laser micro- and nano-structuring of acrylated poly(ethylene glycol) materials and evaluation of their cytoxicity for tissue engineering applications. Acta Biomater **7,** 967, 2011.
41. Lamichhane, S.P., Arya, N., Ojha, N., Kohler, E., and Shastri, V.P. Glycosaminoglycan-functionalized polylactide-co-glycolide nanoparticles: synthesis, characterization, cytocompatibility, and cellular uptake. Int J Nanomed **10,** 775, 2015.
42. Mitsak, A.G., Kemppainen, J.M., Harris, M.T., and Hollister, S.J. Effect of polycaprolactone scaffold permeability on bone regeneration in vivo. Tissue Eng Part A **17,** 1831, 2011.
43. Huang, M.H., Li, S., Hutmacher, D.W., *et al.* Degradation and cell culture studies on block copolymers prepared by ring opening polymerization of epsilon-caprolactone in the presence of poly(ethylene glycol). J Biomed Mater Res A **69,** 417, 2004.
44. Corden, T.J., Jones, I.A., Rudd, C.D., Christian, P., Downes, S., and McDougall, K.E. Physical and biocompatibility properties of poly-epsilon-caprolactone produced using in situ polymerisation: a novel manufacturing technique for long-fibre composite materials. Biomaterials **21,** 713, 2000.
45. Cai, L., and Wang, S.F. Poly(epsilon-caprolactone) acrylates synthesized using a facile method for fabricating networks to achieve controllable physicochemical properties and tunable cell responses. Polymer **51,** 164, 2010.
46. Hoffman, A.S. Hydrogels for biomedical applications. Adv Drug Deliv Rev **54,** 3, 2002.
47. Vertenten, G., Lippens, E., Girones, J., *et al.* Evaluation of an injectable, photopolymerizable, and three-dimensional scaffold based on methacrylate-endcapped poly(D,L-lactide-co-epsilon-caprolactone) combined with autologous mesenchymal stem cells in a goat tibial unicortical defect model. Tissue Eng Part A **15,** 1501, 2009.
48. Lee, K.Y., and Mooney, D.J. Hydrogels for tissue engineering. Chem Rev **101,** 1869, 2001.

49. Gebinoga, M., Katzmann, J., Fernekorn, U., *et al.* Multiphoton structuring of native polymers: a case study for structuring natural proteins. Eng Life Sci **13,** 368, 2013.
50. Huber, B., Borchers, K., Tovar, G.E.M., and Kluger, P.J. Methacrylated gelatin and mature adipocytes are promising components for adipose tissue engineering. J Biomater Appl **30,** 699, 2016.
51. Qin, X.H., Gruber, P., Markovic, M., *et al.* Enzymatic synthesis of hyaluronic acid vinyl esters for two-photon microfabrication of biocompatible and biodegradable hydrogel constructs. Polym Chem-Uk **5,** 6523, 2014.
52. Gupta, V., Mun, G.H., Choi, B.N., *et al.* Repair and reconstruction of a resected tumor defect using a composite of tissue flap-nanotherapeutic-silk fibroin and chitosan scaffold. Ann Biomed Eng **39,** 2374, 2011.
53. Chan, W.P., Kung, F.C., Kuo, Y.L., Yang, M.C., and Lai, W.F.T. Alginate/poly(gamma-glutamic acid) base biocompatible gel for bone tissue engineering. Biomed Res Int **1,** 2015.
54. Hutmacher, D.W. Biomaterials offer cancer research the third dimension. Nat Mater **9,** 90, 2010.
55. Fang, J.Y., Tan, S.J., Yang, Z., Tayag, C., and Han, B. Tumor bioengineering using a transglutaminase crosslinked hydrogel. PLoS One **9,** 1, 2014.
56. Lee, H.J., Ahn, S.H., and Kim, G.H. Three-dimensional collagen/alginate hybrid scaffolds functionalized with a Drug Delivery System (DDS) for bone tissue regeneration. Chem Mater **24,** 881, 2012.
57. Demina, T.S., Zaytseva-Zotova, D.S., Timashev, P.S., *et al.* Chitosan-g-lactide copolymers for fabrication of 3D scaffolds for tissue engineering. Iop Conf Ser-Mat Sci **87,** 1, 2015.
58. Kufelt, O., El-Tamer, A., Sehring, C., Meissner, M., Schlie-Wolter, S., and Chichkov, B.N. Water-soluble photopolymerizable chitosan hydrogels for biofabrication via two-photon polymerization. Acta Biomater **18,** 186, 2015.
59. Kumbar, S.G., Toti, U.S., Deng, M., *et al.* Novel mechanically competent polysaccharide scaffolds for bone tissue engineering. Biomed Mater **6,** 1, 2011.
60. Chicurel, M.E., Chen, C.S., and Ingber, D.E. Cellular control lies in the balance of forces. Curr Opin Cell Biol **10,** 232, 1998.
61. Seppala, J., Korhonen, H., Hakala, R., and Malin, M. Photocrosslinkable polyesters and poly(ester anhydride)s for biomedical applications. Macromol Biosci **11,** 1647, 2011.
62. Engler, A.J., Sen, S., Sweeney, H.L., and Discher, D.E. Matrix elasticity directs stem cell lineage specification. Cell **126,** 677, 2006.
63. Russias, J., Saiz, E., Nalla, R.K., Gryn, K., Ritchie, R.O., and Tomsia, A.P. Fabrication and mechanical properties of PLA/HA composites: a study of in vitro degradation. Mater Sci Eng C Biomim Supramol Syst **26,** 1289, 2006.
64. Shimko, D.A., and Nauman, E.A. Development and characterization of a porous poly(methyl methacrylate) scaffold with controllable modulus and permeability. J Biomed Mater Res B **80b,** 360, 2007.
65. Baker, E.L., Srivastava, J., Yu, D., Bonnecaze, R.T., and Zaman, M.H. Cancer cell migration: integrated roles of matrix mechanics and transforming potential. PLoS One **6,** 1, 2011.
66. Buxboim, A., Ivanovska, I.L., and Discher, D.E. Matrix elasticity, cytoskeletal forces and physics of the nucleus: how deeply do cells ''feel'' outside and in?. J Cell Sci **123,** 297, 2010.
67. Janmey, P.A., Winer, J.P., Murray, M.E., and Wen, Q. The hard life of soft cells. Cell Motil Cytoskel **66,** 597, 2009.
68. Meretoja, V.V., Helminen, A.O., Korventausta, J.J., Haapa-aho, V., Seppala, J.V., and Narhi, T.O. Crosslinked poly(epsilon-caprolactone/D,L-lactide)/bioactive glass composite scaffolds for bone tissue engineering. J Biomed Mater Res A **77,** 261, 2006.
69. Felfel, R.M., Poocza, L., Gimeno-Fabra, M., *et al.* In vitro degradation and mechanical properties of PLA-PCL copolymer unit cell scaffolds generated by two-photon polymerization. Biomed Mater **11,** 1, 2016.
70. Grohmann, S., Rothe, H., Frant, M., and Liefeith, K. Colloidal force spectroscopy and cell biological investigations on biomimetic polyelectrolyte multilayer coatings composed of chondroitin sulfate and heparin. Biomacromolecules **12,** 1987, 2011.
71. Morand, D.N., Huck, O., Keller, L., Jessel, N., Tenenbaum, H., and Davideau, J.L. Active nanofibrous membrane effects on gingival cell inflammatory response. Materials **8,** 7217, 2015.
72. Mehr, N.G., Li, X., Chen, G., Favis, B.D., and Hoemann, C.D. Pore size and LbL chitosan coating influence mesenchymal stem cell in vitro fibrosis and biomineralization in 3D porous poly(epsilon-caprolactone) scaffolds. J Biomed Mater Res A **103,** 2449, 2015.
73. Gai, M.Y., Frueh, J., Girard-Egrot, A., Rebaud, S., Doumeche, B., and He, Q. Micro-contact printing of PEM thin films: effect of line tension and surface energies. RSC Adv **5,** 51891, 2015.
74. Sailer, M., Sun, K.L.W., Mermut, O., Kennedy, T.E., and Barrett, C.J. High-throughput cellular screening of engineered ECM based on combinatorial polyelectrolyte multilayer films. Biomaterials **33,** 5841, 2012.
75. Picart, C., Caruso, F., and Voegel, J.C. Layer-by-Layer Films for Biomedical Applications. Weinheim, Germany: Whiley VCH 2015.
76. Guzman, E., Maestro, A., Llamas, S., *et al.* 3D solid supported inter-polyelectrolyte complexes obtained by the alternate deposition of poly(diallyldimethylammonium chloride) and poly(sodium 4-styrenesulfonate). Beilstein J Nanotechnol **7,** 197–208, 2016.
77. Dodoo, S., Steitz, R., Laschewsky, A., and von Klitzing, R. Effect of ionic strength and type of ions on the structure of water swollen polyelectrolyte multilayers. Phys Chem Chem Phys **13,** 10318–10325, 2011.
78. Chung, T.W., Lu, Y.F., Wang, S.S., Lin, Y.S., and Chu, S.H. Growth of human endothelial cells on photochemically grafted Gly-Arg-Gly-Asp (GRGD) chitosans. Biomaterials **23,** 4803, 2002.
79. Li, B., Chen, J., and Wang, J.H. RGD peptide-conjugated poly(dimethylsiloxane) promotes adhesion, proliferation, and collagen secretion of human fibroblasts. J Biomed Mater Res A **79,** 989, 2006.
80. Connelly, J.T., Petrie, T.A., Garcia, A.J., and Levenston, M.E. Fibronectin- and collagen-mimetic ligands regulate bone marrow stromal cell chondrogenesis in three-dimensional hydrogels. Eur Cell Mater **22,** 168, 2011.
81. Nishitani, W.S., Alencar, A.M., and Wang, Y. Rapid and localized mechanical stimulation and adhesion assay: TRPM7 involvement in calcium signaling and cell adhesion. PLoS One **10,** 1, 2015.

82. Yip, A.K., Iwasaki, K., Ursekar, C., *et al.* Cellular response to substrate rigidity is governed by either stress or strain. Biophys J **104,** 19, 2013.
83. Ye, Z., and Zhao, X. Phase imaging atomic force microscopy in the characterization of biomaterials. J Microsc **238,** 27, 2010.
84. Sittichokechaiwut, A., Edwards, J.H., Scutt, A.M., and Reilly, G.C. Short bouts of mechanical loading are as effective as dexamethasone at inducing matrix production by human bone marrow mesenchymal stem cell. Eur Cell Mater **20,** 45, 2010.
85. Chan, B.P., and Leong, K.W. Scaffolding in tissue engineering: general approaches and tissue-specific considerations. Eur Spine J **17 Suppl 4,** 467, 2008.
86. Biggs, M., Pandit, A., and Zeugolis, D.I. 2D imprinted substrates and 3D electrospun scaffolds revolutionize biomedicine. Nanomedicine (Lond) **11,** 989, 2016.
87. Hamlekhan, A., Moztarzadeh, F., Mozafari, M., Azami, M., and Nezafati, N. Preparation of laminated poly(epsilon-caprolactone)-gelatin-hydroxyapatite nanocomposite scaffold bioengineered via compound techniques for bone substitution. Biomatter **1,** 91, 2011.
88. Owen, R., Sherborne, C., Paterson, T., Green, N.H., Reilly, G.C., and Claeyssens, F. Emulsion templated scaffolds with tunable mechanical properties for bone tissue engineering. J Mech Behav Biomed **54,** 159, 2016.
89. Scaglione, S., Lazzarini, E., Ilengo, C., and Quarto, R. A composite material model for improved bone formation. J Tissue Eng Regen M **4,** 505, 2010.
90. Torabinejad, B., Mohammadi-Rovshandeh, J., Davachi, S.M., and Zamanian, A. Synthesis and characterization of nanocomposite scaffolds based on triblock copolymer of L-lactide, epsilon-caprolactone and nano-hydroxyapatite for bone tissue engineering. Mater Sci Eng C Mater Biol Appl **42,** 199, 2014.
91. Choi, J.S., Lee, S.J., Christ, G.J., Atala, A., and Yoo, J.J. The influence of electrospun aligned poly(epsilon-caprolactone)/collagen nanofiber meshes on the formation of self-aligned skeletal muscle myotubes. Biomaterials **29,** 2988, 2008.
92. Wang, J., Li, D.S., Li, T.Y., *et al.* Gelatin tight-coated poly(lactide-co-glycolide) scaffold incorporating rhBMP-2 for bone tissue engineering. Materials **8,** 1009, 2015.
93. Hutmacher, D.W., Schantz, T., Zein, I., Ng, K.W., Teoh, S.H., and Tan, K.C. Mechanical properties and cell cultural response of polycaprolactone scaffolds designed and fabricated via fused deposition modeling. J Biomed Mater Res **55,** 203, 2001.
94. Pang, Y., Horimoto, Y., Sutoko, S., *et al.* Novel integrative methodology for engineering large liver tissue equivalents based on three-dimensional scaffold fabrication and cellular aggregate assembly. Biofabrication **8,** 1, 2016.
95. Yang, N., Tian, Y.L., and Zhang, D.W. Novel real function based method to construct heterogeneous porous scaffolds and additive manufacturing for use in medical engineering. Med Eng Phys **37,** 1037, 2015.
96. Weiss, T., Schade, R., Laube, T., *et al.* Two-photon polymerization of biocompatible photopolymers for microstructured 3D biointerfaces. Adv Eng Mater **13,** B264, 2011.
97. Stratakis, E., Ranella, A., Farsari, M., and Fotakis, C. Laser-based micro/nanoengineering for biological applications. Prog Quant Electron **33,** 127, 2009.
98. Gittard, S.D., and Narayan, R. Laser direct writing of micro- and nano-scale medical devices. Expert Rev Med Devic **7,** 343, 2010.
99. Ciuciu, A.I., and Cywinski, P.J. Two-photon polymerization of hydrogels—versatile solutions to fabricate well-defined 3D structures. RSC Adv **4,** 45504, 2014.
100. Lee, J.W. 3D nanoprinting technologies for tissue engineering applications. J Nanomater **1,** 2015.
101. Murr, L.E., Gaytan, S.M., Martinez, E., Medina, F., and Wicker, R.B. Next generation orthopaedic implants by additive manufacturing using electron beam melting. Int J Biomater **2012,** 1, 2012.
102. Afshar, M., Anaraki, A.P., Montazerian, H., and Kadkhodapour, J. Additive manufacturing and mechanical characterization of graded porosity scaffolds designed based on triply periodic minimal surface architectures. J Mech Behav Biomed **62,** 481, 2016.
103. Blanquer, S.B.G., Werner, M., Hannula, M., *et al.* Surface curvature in triply-periodic minimal surface architectures as a distinct design parameter in preparing advanced tissue engineering scaffolds. Biofabrication **9,** 1, 2017.
104. Fantani, M., Curto, M., and De Crescenzio, F. TPMS for interactive modeling of trabecular scaffolds for bone tissue engineering. In: Kwon, Y.W., Chaari, F., Haddar, M., Di Cecco, L., and Shen, L., eds. Lecture Notes in Mechanical Engineering. Berlin, Germany: Springer, 2017, pp. 425–435.
105. Rajagopalan, S., and Robb, R.A. Schwarz meets Schwann: design and fabrication of biomorphic and durataxic tissue engineering scaffolds. Med Image Anal **10,** 693, 2006.
106. Petrochenko, P.E., Torgersen, J., Gruber, P., *et al.* Laser 3D printing with sub-microscale resolution of porous elastomeric scaffolds for supporting human bone stem cells. Adv Healthc Mater **4,** 739, 2015.
107. Psycharakis, S., Tosca, A., Melissinaki, V., Giakoumaki, A., and Ranella, A. Tailor-made three-dimensional hybrid scaffolds for cell cultures. Biomed Mater **6,** 1, 2011.
108. Aprile, V., Eaton, S.M., Lagana, M., Cerullo, G., Raimondi, M.T., and Osellame, R. Femtosecond laser two-photon polymerization of three-dimensional scaffolds for tissue engineering and regenerative medicine applications. Proc Spie **8247,** 1, 2012.
109. Almeida, H.A., and Bartolo, P.J. Tensile and shear stress evaluation of schwartz surfaces for scaffold design. Procedia Eng **110,** 167, 2015.
110. Ambu, R., and Morabito, A.E. Design and analysis of tissue engineering scaffolds based on open porous non-stochastic cells. Lect N Mech Eng 777, 2017.
111. Piola, M., Soncini, M., Cantini, M., Sadr, N., Ferrario, G., and Fiore, G.B. Design and functional testing of a multi-chamber perfusion platform for three-dimensional scaffolds. Sci World J **1,** 2013.
112. Allori, A.C., Davidson, E., Reformat, D.D., *et al.* Design and validation of a dynamic cell-culture system for bone biology research and exogenous tissue-engineering applications. J Tissue Eng Regen M **10,** E327, 2016.
113. Haykal, S., Salna, M., Zhou, Y.Z., *et al.* Double-chamber rotating bioreactor for dynamic perfusion cell seeding of large-segment tracheal allografts: comparison to conventional static methods. Tissue Eng Part C-Me **20,** 681, 2014.

114. Kreke, M.R., Sharp, L.A., Lee, Y.W., and Goldstein, A.S. Effect of intermittent shear stress on mechanotransductive signaling and osteoblastic differentiation of bone marrow stromal cells. Tissue Eng Part A **14,** 529, 2008.
115. Chouinard, J.A., Gagnon, S., Couture, M.G., Levesque, A., and Vermette, P. Design and validation of a pulsatile perfusion bioreactor for 3D high cell density cultures. Biotechnol Bioeng **104,** 1215, 2009.
116. Anisi, F., Salehi-Nik, N., Amoabediny, G., Pouran, B., Haghighipour, N., and Zandieh-Doulabi, B. Applying shear stress to endothelial cells in a new perfusion chamber: hydrodynamic analysis. J Artif Organs **17,** 329, 2014.
117. Sapudom, J., Rubner, S., Martin, S., *et al.* The phenotype of cancer cell invasion controlled by fibril diameter and pore size of 3D collagen networks. Biomaterials **52,** 367, 2015.
118. Yilgor, P., Sousa, R.A., Reis, R.L., Hasirci, N., and Hasirci, V. 3D plotted PCL scaffolds for stem cell based bone tissue engineering. Macromol Symp **269,** 92, 2008.
119. Raimondi, M.T., Nava, M.M., Eaton, S.M., *et al.* Optimization of femtosecond laser polymerized structural niches to control mesenchymal stromal cell fate in culture. Micromachines-Basel **5,** 341, 2014.
120. American Cancer Society, Global Cancer Facts & Figures, 4th Edition, 2018.
121. Chaffer, C.L., and Weinberg, R.A. A perspective on cancer cell metastasis. Science **331,** 1559, 2011.
122. Chen, Y.C., Allen, S.G., Ingram, P.N., Buckanovich, R., Merajver, S.D., and Yoon, E. Single-cell migration chip for chemotaxis-based microfluidic selection of heterogeneous cell populations. Sci Rep **5,** 1, 2015.
123. Singh, S.P., Schwartz, M.P., Tokuda, E.Y., *et al.* A synthetic modular approach for modeling the role of the 3D microenvironment in tumor progression. Sci Rep **5,** 1, 2015.
124. Lühmann, T., and Hall, H. Cell guidance by 3D-gradients in hydrogel matrices: importance for biomedical applications. Materials **2,** 1058, 2009.
125. Discher, D.E., Janmey, P., and Wang, Y.L. Tissue cells feel and respond to the stiffness of their substrate. Science **310,** 1139, 2005.
126. Keely, P.J. Mechanisms by which the extracellular matrix and integrin signaling act to regulate the switch between tumor suppression and tumor promotion. J Mammary Gland Biol **16,** 205, 2011.
127. Balachander, G.M., Balaji, S.A., Rangarajan, A., and Chatterjee, K. Enhanced metastatic potential in a 3D tissue scaffold toward a comprehensive in vitro model for breast cancer metastasis. Acs Appl Mater Inter **7,** 27810, 2015.
128. Blanco, T.M., Mantalaris, A., Bismarck, A., and Panoskaltsis, N. The development of a three-dimensional scaffold for ex vivo biomimicry of human acute myeloid leukaemia. Biomaterials **31,** 2243, 2010.
129. Pranav, S., Kelber, J.A., Lee, J.W., *et al.* Cancer cell migration within 3D layer-by-layer microfabricated photocrosslinked PEG scaffolds with tunable stiffness. Biomaterials **33,** 7064, 2012.
130. Engelhardt, S., Hoch, E., Borchers, K., *et al.* Fabrication of 2D protein microstructures and 3D polymer-protein hybrid microstructures by two-photon polymerization. Biofabrication **3,** 1, 2011.
131. Bulysheva, A.A., Bowlin, G.L., Petrova, S.P., and Yeudall, W.A. Enhanced chemoresistance of squamous carcinoma cells grown in 3D cryogenic electrospun scaffolds. Biomed Mater **8,** 1, 2013.
132. Rao, S.S., Nelson, M.T., Xue, R.P., *et al.* Mimicking white matter tract topography using core-shell electrospun nanofibers to examine migration of malignant brain tumors. Biomaterials **34,** 5181, 2013.
133. Jin, H., Pi, J., Huang, X., *et al.* BMP2 promotes migration and invasion of breast cancer cells via cytoskeletal reorganization and adhesion decrease: an AFM investigation. Appl Microbiol Biotechnol **93,** 1715, 2012.
134. Ponta, H., Sherman, L., and Herrlich, P.A. CD44: from adhesion molecules to signalling regulators. Nat Rev Mol Cell Biol **4,** 33, 2003.
135. Reichert, J.C., Wullschleger, M.E., Cipitria, A., *et al.* Custom-made composite scaffolds for segmental defect repair in long bones. Int Orthop **35,** 1229–1236, 2011.
136. Zhang, B., and Radisic, M. Organ-on-a-chip devices advance to market. Lab Chip **17,** 2395, 2017.
137. Kilic, T., Navaee, F., Stradolini, F., Renaud, P., and Carrara, S. Organs-on-chip monitoring: sensors and other strategies. Microphysiological Syst **2,** 1, 2018.

Address of correspondence
*Klaus Liefeith, PhD*
*Department of Biomaterials*
*Institute for Bioprocessing and Analytical Measurement Techniques e.V. (iba)*
*Rosenhof*
*Heilbad Heiligenstadt 37308*
*Germany*

*E-mail:* klaus.liefeith@iba-heiligenstadt.de

*Received: September 28, 2018*
*Accepted: January 1, 2019*
*Online Publication Date: May 5, 2019*